

Exhibit 107

Part 1

**IN RE JOHNSON & JOHNSON TALCUM POWDER PRODUCTS
MARKETING, SALES PRACTICES, AND PRODUCTS LIABILITY
LITIGATION
MDL NO. 16-2738 (FLW) (LHG)**

Shu-Chun Su

2024-05-21

Credentials

My name is Shu-Chun Su. I have developed methods and published on issues related to the identification of asbestos by polarized light microscopy (PLM) throughout my more than forty-year career.

I was born in China. I majored in Geochemistry at the Department of Geology, Peking University, for my bachelor's, a six-year program mirroring science programs at Moscow University. My Optical Crystallography was a two-semester (40 weeks) course. So was Optical Mineralogy. These two courses are the foundations of identifying rock-forming minerals using PLM. American Geology departments teach these two subjects in several weeks, not as complete semester courses. I graduated from Peking University in 1964, and I worked as a geological engineer in the Geological Survey of Gansu Province of China for 14 years. My job was to identify rock and mineral samples collected by field geologists in the geological mapping of the Gansu Province using a Zeiss polarized light microscope. Serpentine asbestos (chrysotile) was a common mineral species among the field samples of ultramafic rocks in that area. I developed expertise in the identification of asbestos—and specifically chrysotile—during my work here.

In 1979, I attended the Institute of Geology, Chinese Academy of Science, for graduate studies and obtained my Master's Degree in Mineralogy in 1981. Then, I came to the United States to pursue my doctoral studies at Virginia Institute of Technology and State University under Professor Donald Bloss, the preeminent, world-renowned expert in optical crystallography. My doctoral thesis was the study of silicate minerals by light and electron microscopy and X-ray diffraction spectroscopy, which are the same techniques used to analyze asbestos. The identification of chrysotile and other asbestos minerals by light microscopy is something that I have been researching and publishing for more than forty years.

After obtaining my Ph.D. in geology in 1985, I did two years of postdoctoral research in the development of an automatic optical instrument for measuring minerals' refractive index invented by Professor Bloss. I went to work at the Research Center, Hercules Incorporated, a specialty chemical and aerospace company. I was the director of the Optical and Electron Microscopy Laboratory in Wilmington, Delaware. My job was to characterize materials produced and researched by the company using various optical and electron microscopy techniques. As part of this work, I characterized chrysotile and other types of asbestos by PLM.

In 1988, I was recruited to become a Technical Expert in the Bulk and Airborne Asbestos Programs by the National Voluntary Laboratory Accreditation Program (NVLAP) under the Department of Commerce, a government office regulating asbestos analysis laboratories. Since then, I've conducted approximately one thousand on-site audits of asbestos laboratories, mainly in the United States but also in Canada, Japan, and Korea. These audits assess the laboratories' managerial and

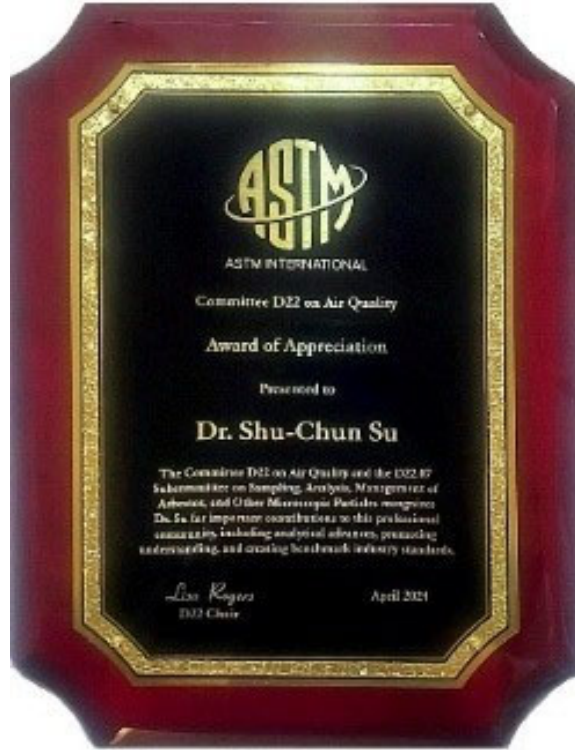
technical proficiency in conducting standardized PLM and TEM asbestos analyses. Every asbestos laboratory with (or seeking) NVLAP accreditation performs PLM asbestos analyses.

To date, I've authored 29 publications on asbestos analysis, which are identified in my biography, which is attached as **Exhibit A**.

In the area of airborne asbestos analysis, I have created 880 pages of comprehensive tables for the identification of amphibole asbestos, which has been widely used by airborne asbestos laboratories around the world.

My most well-known contribution to asbestos analysis is a standard operating procedure to quickly and accurately measure the refractive index (RI) of asbestos minerals (the primary diagnostic optical property of “fingerprinting” asbestos minerals) using the central stop dispersion staining technique by PLM. This procedure is accurate and highly efficient, reducing a lengthy ten-minute graphic solution of RI value into 10 seconds. This technique has been referred to as the “Su Method” by scientists practicing in this area and has been cited in textbooks addressing the identification of asbestos by PLM. The Su Method has been adopted by most analytical laboratories performing PLM analyses in the United States and overseas. In fact, Dr. William Longo’s laboratory MAS reports that they themselves have been using my Su Method for Johnson’s Baby Powder analyses.

In April 2024, at ASTM International’s Michael Beard Conference on Asbestos Terminology, the organization presented me with an award recognizing my career-long contributions to asbestos analysis, including recognizing the “Su Method” as a significant achievement in PLM analytical procedures.



As noted above, I am an accomplished expert in the characterization of asbestos minerals by PLM. It has been a focus of my entire career. As such, I am uniquely qualified to assess whether or not a laboratory's PLM data identifying asbestos using my Su Method is reliable and accurate.

Scope of Analysis

I have been asked to review PLM data put forth by Dr. Longo's laboratory MAS in which he claims to identify "chrysotile" in Johnson's Baby Powder by PLM using central stop dispersion staining. I am being compensated at a rate of \$800 per hour for my scientific analysis of this issue. I have not provided any deposition or trial testimony in the past four years.

A list of the MAS reports that I reviewed identifying "chrysotile" in Johnson's Baby Powder is identified in **Exhibit B**.

As I explain further below, I disagree with each and every single PLM identification of "chrysotile" in Johnson's Baby Powder made by Dr. Longo's laboratory in the reports that I have reviewed. The data presented by MAS demonstrate significant deficiencies in all areas, which leads me to conclude that the laboratory is incapable of performing the most fundamental aspects of PLM analysis or correctly identifying chrysotile by PLM. A summary of the analytical failings of MAS appears below and is expanded upon in the demonstrative materials that I have attached as **Exhibit C**. The bases for my opinions are my experience, education, training, my publications that are listed in **Exhibit A**, and the sources cited in this report and the attached **Exhibit C**.

Summary of Analysis

Dr. Longo's laboratory's identification of "chrysotile" in Johnson's Baby Powder by PLM is incorrect and unreliable for the following reasons:

1. MAS's Procedure for Measuring Refractive Index Values is Inaccurate and Unreliable

a. MAS Used Suppressed Light Intensity, Leading to Inaccurate and Unreliable Refractive Index Value Determination

In order to accurately measure the RI value of a mineral by PLM, it is fundamental that the equipment used needs to be set appropriately. MAS routinely uses insufficient light intensity, as if the light intensity was suppressed, which in turn subdues the dispersion staining color, resulting in a subdued RI value and a subdued birefringence value. The result is that talc's high γ and the associated birefringence are suppressed, making the elongated talc particle look like chrysotile. If the light suppression is unintentional, then MAS has failed to conduct basic PLM procedures, such as adjusting the light intensity and aperture diaphragm to optimal condition to achieve a fully and adequately displayed dispersion staining color or accurately calibrating the objective lens so that it can measure particles size accurately (as I will discuss further below).

I describe examples of this problem on pages 2 through 5 of **Exhibit C**.

b. Inaccurate Refractive Index Measurement Procedure Leads to Unreliable Results

MAS routinely fails to accurately identify the RI value exhibited by particles in its PLM analyses. There are numerous instances of MAS assigning an RI value that is simply wrong (and incorrectly closer to values that may be associated with chrysotile rather than talc). Based on my review of the reports identified in **Exhibit B**, the data presented by MAS demonstrates a systematic failure to assign RI values correctly. I describe examples of this systematic problem on pages 6 through 11 of **Exhibit C**.

In addition, there are other instances in which a talc particle exhibits a distorted dispersion staining color due to the total reflection occurring at the liquid-solid interface that a proficient PLM analyst who understands the basic principles of the central stop dispersion staining technique would recognize as a common phenomenon. Instead, MAS used the distorted dispersion staining color for RI assignments, leading to incorrect RI value, which, in turn, led to the misidentification of talc particles as “chrysotile.” I describe examples of this problem on pages 12 through 14 of **Exhibit C**.

c. Dr. Longo's Claim That Particle Sizes Change Refractive Index Values Is Wrong

A mineral’s RI is a constant governed by their chemical composition and crystal structure. MAS’s theory that chrysotile’s RI increases as the particle size decreases is unfounded and defies basic principles of physics. In fact, if such a theory is proved, it would shake the very foundation of physics.

The National Institute of Standards and Technology (NIST) Standard Reference Material (SRM) 1866 chrysotile RI values, α 1.549 and γ 1.556, were measured by John Phelps, a scientist at NIST, on a single fiber using the spindle stage technique. I know these details because John Phelps was in communication with me during the measurements that became the published SRM reference values. The spindle stage technique was invented by Professor Donald Bloss, my Ph.D. supervisor. I am an expert in this technique and author of the computer program used in the spindle stage measurement procedure. The “chrysotile” fibers that MAS claims to identify in Johnson’s Baby Powder by PLM cannot be any thinner than the NIST SRM 1866 single chrysotile fiber that serves as the data point for the certified RI values for this material. MAS’s claim that the particle sizes of “chrysotile” it finds in PLM analyses of Johnson’s Baby Powder are so unique is not only unfounded but also without the support of credible measurement data that directly refutes the claim. I describe this problem on pages 15 and 16 of **Exhibit C**.

Another critical fact is that certified NVLAP RI values of “Calidria” chrysotile—a unique form of chrysotile from California that MAS claims is similar to the “chrysotile” it finds by PLM in Johnson’s Baby Powder—are α 1.555 and γ 1.560, which are only 0.004 - 0.006 higher than the SRM 1866 chrysotile, documented by NVLAP in “ANALYSIS SUMMARY FOR NIST BULK ASBESTOS PROFICIENCY TESTING February 2001, Test Round M12001.” Again, MAS’s claim that the particle sizes and RI values of the “chrysotile” it found in PLM analyses of Johnson’s Baby Powder are a match for Calidria chrysotile are inaccurate and not supported by the data. I describe this problem on page 17 of **Exhibit C**.

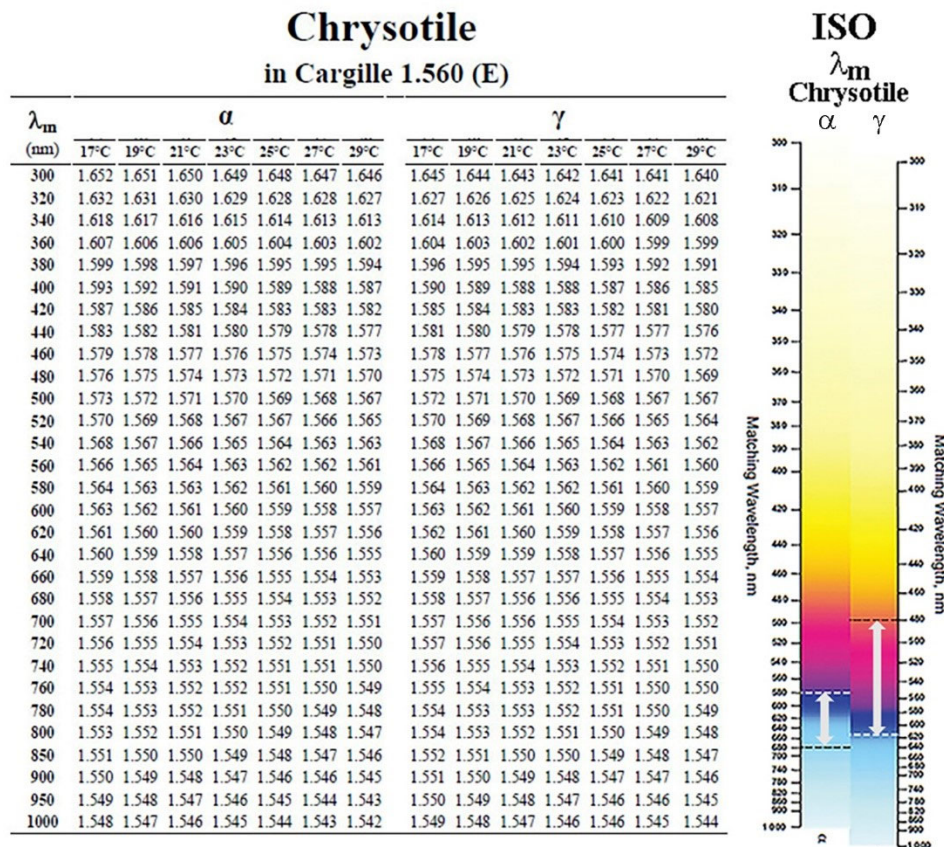
d. MAS's Complete Misunderstanding of My Central Stop Dispersion Staining Color Conversion Tables Leads to Incorrect and Unreliable "Chrysotile" Identification

I have created and published procedures and reference tables that help analysts measure RI values of the six regulated asbestos minerals, including chrysotile. MAS relies upon my procedure and tables as part of its PLM analyses of Johnson's Baby Powder.

However, Dr. Longo completely misunderstood my reference table and claimed that the RI range of my chrysotile table represents the chrysotile's minimum and maximum RI values. This is not true.

To illustrate, in the International Organization for Standardization (ISO) chart included in the 22262-1 method, the possible α and γ RI ranges of chrysotile are only a small section (between the dotted lines in the following figure) of the dispersion staining color chart; the chart must cover the whole dispersion staining color spectrum, and the same is true of my conversion table. The ranges of the ISO chart and my table must be much wider than the RI range of chrysotile.

My table is the numerical version of the ISO graphic chart for people who understand the principle. For people who do not understand this basic principle of my procedure and tables, it is impossible to correctly perform the analytical procedure of RI measurement by dispersion staining technique.



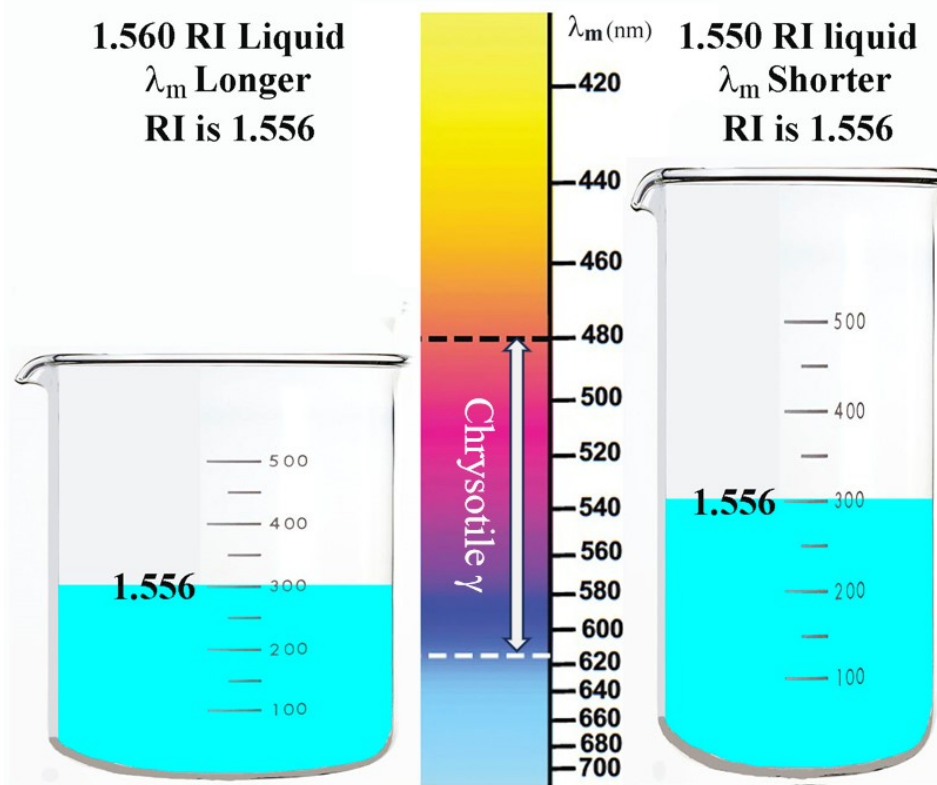
I describe this problem on pages 18 through 20 of **Exhibit C**.

e. Dr. Longo's Understanding of the Refractive Index Liquid's Effect on Mineral's Refractive Index Values Is Wrong

In 2022, I published a paper on the application of the dispersion staining technique to asbestos analysis. I recommended the use of 1.560 RI liquid for measuring the γ of Calidria chrysotile to improve the accuracy of measurement.

The only purpose of switching from 1.550 to 1.560 is to improve the accuracy of RI measurement because chrysotile's RI is a constant and does not change with the surrounding liquid medium.

When the same mineral is measured in two different RI liquids, its RI remains the same, but the matching wavelength λ_m changes accordingly: the lower liquid produces a shorter λ_m and the higher liquid produces a longer λ_m .



The above diagram shows two beakers; the left one is wider, representing 1.560 liquid, and the right one is thinner, representing 1.550 liquid. The volume of water represents the γ refractive index.

The 300 milliliters of water volume – γ value – does not change, but the water level – λ_m – changes from a shorter (upper) matching wavelength to a longer (lower) matching wavelength.

In 2022, Dr. Longo switched to 1.560 RI liquid. Without any background in optical crystallography, he mistakenly thought measuring in the 1.560 RI liquid would give his laboratory results different from those using 1.550 RI liquid. As noted below, MAS's use of the 1.560 RI liquid produced a suite of α and γ values similar to the 1.550 RI liquid values, none of which establish the

presence of chrysotile.

M71614-M71643-M71740 J&J Baby Powders

Date	MAS No.			γ		α				
				Low	High	Low	High			
2023-02-28	M71614	001	1	1.564	1.564	1.561	1.561			
				2	1.565	1.565	1.561			
				3	1.568	1.568	1.557			
				4	1.565	1.568	1.560			
2023-10-19	M71643	001	1	1.566	1.566	1.561	1.561			
				2	1.566	1.569	1.557			
				3	1.561	1.561	1.552			
				4	1.568	1.568	1.559			
2024-02-15	M71740	001	1	1.564	1.564	1.560	1.560			
				2	1.564	1.564	1.560			
				3	1.565	1.565	1.562			
				4	1.563	1.563	1.561			
				Average	1.565	1.565	1.559			
				Grand Average	1.565		1.560			

The above table summarizes 12 pairs of α and γ values from 2023 (M71614 and M71643) and 2024 (M71740) reports.

Three Types of Chrysotile

Type	α	γ	Birefringence	RI	Source
SRM 1866	1.549	1.556	0.007	Standard	NIST
Calidria	1.555	1.560	0.005	Significantly higher than 1866	NVLAP
New?	1.560*	1.565*	0.005	Significantly higher than Calidria	MAS

* Average of 12 samples in M71614, M71643, and M71740.

When I used the term “significantly higher” to describe Calidria chrysotile as compared to NIST SRM 1866 chrysotile, the RI values were in the area of .006 to .004 higher as described above. MAS’s “chrysotile” is another “significantly higher” increase above Calidria chrysotile. Were those data credible (and they are not), MAS single-handedly discovered a new type of chrysotile, whose RI is significantly higher than the Calidria chrysotile as shown in the above table. Obviously, there has never been any report of the existence of such a unique type of chrysotile with such peculiar optical properties. MAS is simply wrong again.

I describe this problem on pages 21 and 22 of **Exhibit C**.

2. MAS's Procedure for Measuring Particle Sizes is Inaccurate and Unreliable

a. Scale Bars Are Completely Inaccurate

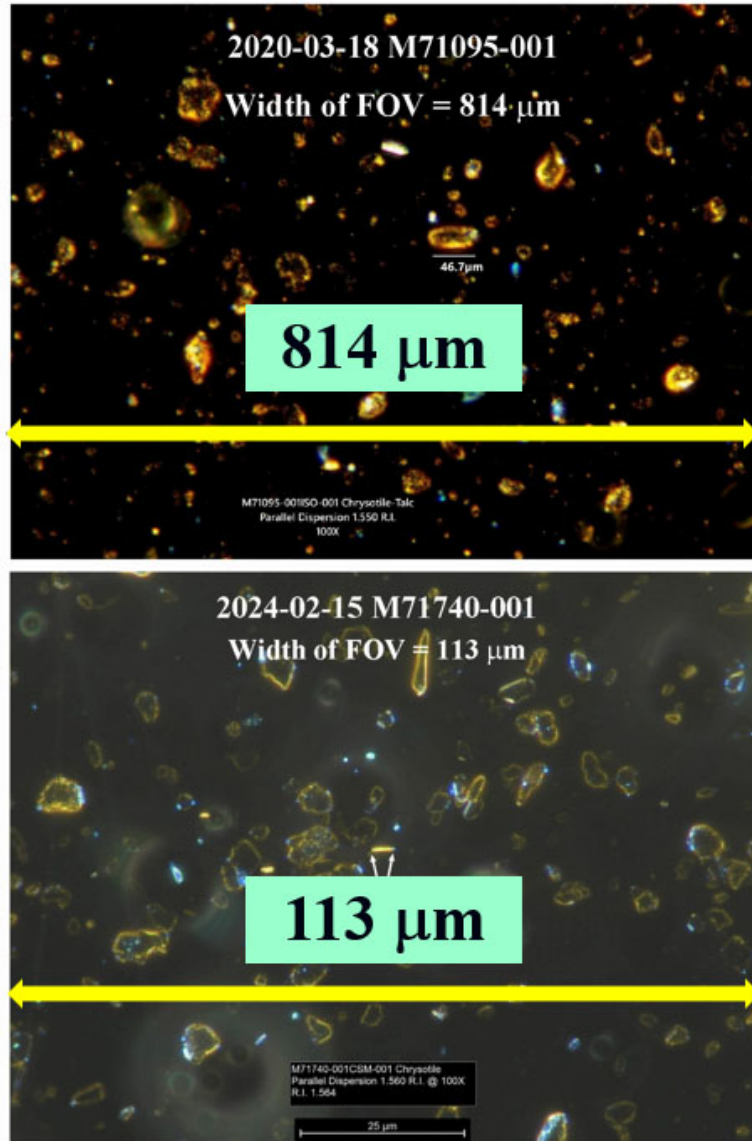
Mineral	Minimum (μm)	Average (μm)	Maximum (μm)	Reference
Talc	1.5	9.3	37.0	MAS (2017)
SG-210 Chrysotile	3.0	8.0	10.0	MAS (2023)

MAS reported the above talc particle size data from analyzing approximately 30 containers of Johnson & Johnson talcum powder products by SEM using image analysis software in 2017. The maximum particle size is 37 micrometers, which makes sense because the specification of Baby Powder is passing through a 325 mesh (44 micrometers) sieve.

Date	MAS No.	Chrysotile Length (μm)		
		Individual	Average	vs. Talc
2020-02-24 M70484	001-001	78.8	61.6	Same particle size range as talc
	001-002	33.3		
	001-003	38.5		
	001-004	71.3		
	001-005	62.2		
	001-006	57.0		
	001-007	70.4		
	001-008	49.6		
	002-001	58.5		
	002-002	78.5		
2020-03-18 M71095	002-003	79.3		
	001-001	46.7	32.2	Same particle size range as talc
	001-002	13.3		
	001-003	34.8		
2020-03-20 M70877	001-004	34.1		
	001-001	60.0	37.6	Same particle size range as talc
	001-002	25.9		
	001-003	23.0		
2021-05-25 M71228	001-004	41.5		
	001-001	105.2	55.2	Same particle size range as talc
	001-002	59.5		
	001-003	17.2		
2022-03-11 M71262	001-004	38.8		
	001-001	32.8	32.8	Same particle size range as talc
	001-002	21.6		
	001-003	26.7		
2023-03-28 M71614	001-004	50.0	4.9	Same particle size range as talc
	001-001	6.0		
	001-002	5.1		
	001-003	3.9		
2023-10-19 M71643	001-004	4.8	3.8	Same particle size range as talc
	001-001	3.9		
	001-002	6.6		
	001-003	2.2		
2024-02-15 M71740	001-004	2.7	8.5	Same particle size range as talc
	001-001	3.6		
	001-002	9.4		
	001-003	12.0		
	001-004	8.9		

The above table summarizes eight reports over the last five years. The dramatic variation of the “chrysotile” particle size, which is in the same size ranges as talc that can be seen in the PLM photomicrographs in each of the above reports, clearly indicates inaccurate scale bars, leading to inaccurate particle size measurements.

The creation of an accurate scale bar is a fundamental (and normally very easy) procedure of PLM. Over the years, MAS’s systematic failure to create accurate scale bars for their analyses of Johnson’s Baby Powder by PLM can only be attributed to the lack of basic expertise of MAS’s analysts.



The width of the field of view (FOV) can be calculated from the scale bar length or the width of an object in the image. In the March 18, 2020 report M71095, the 814 μm field of view (FOV) width was wrong. Five years later, the mistake remained uncorrected. The February 15, 2024 report M71228 still reported a grossly wrong FOV width of 113 μm . Regardless of the microscope’s make, Olympus

Nikon Leitz or Leica, the FOV width for a 10X objective lens is slightly over 1 mm or 1,000 μm .

What is important is that the particle sizes in these two micrographs with drastically different FOV widths are the same. That is because they are taken at the same magnification but the scales reported by MAS are wrong.

The only conclusion is that MAS is not capable of correctly performing PLM's most fundamental operation procedure: measuring the sizes of particles that it is analyzing. On occasion, the particle sizes are incorrect by ten times or more.

I describe this problem on pages 23 through 25 of **Exhibit C**.

b. If Chrysotile Was Truly Present In Johnson's Baby Powder, Its Particle Sizes Would Not Match Talc, as MAS Claims

Although MAS fails to correctly measure particle size by PLM, the micrographs in every Johnson's Baby Powder analytical report document the undeniable fact that the particle size of the claimed "chrysotile" matches the particle size of the surrounding talc. If that were true, it means the chrysotile's particle size was reduced to the particle size range of talc particles during the milling process of Johnson's Baby Powder production.

Chrysotile is a mineral with a very high tensile strength, around 100,000 pounds per square inch. It is so strong that it used to be woven into fabrics for making heat protection gears used in steel mills. It is also a super anti-abrasion additive used to make automobile braking shoes.

On the other hand, talc is the softest mineral on Earth. It is easily breakable.

The two minerals have drastically different grinding behaviors. When ground together, talc is easily and quickly ground into fine powders, whereas chrysotile is reduced to a particle size of hundreds of micrometers, significantly larger than talc. This differential grinding effect has been confirmed by US Pharmacopeia (2022) and Pier (2017).

Therefore, the "chrysotile" particles within the particle size range of talc powders cannot be chrysotile. They are talc.

I describe this problem on pages 26 through 52 of **Exhibit C**.

3. MAS's Procedure for Reporting Amounts of "Chrysotile" Identified in Johnson's Baby Powder is Inaccurate and Unreliable

a. Visually Estimated Percentages Are Inherently Unreliable

EPA bulk asbestos analysis procedure requires a point counting procedure for the asbestos quantification. The visual estimate procedure cannot quantify asbestos concentration at 0.00x% level, let alone 0.000x% level. NVLAP requires calibrated visual estimates (CVEs) for quantifying asbestos by PLM at the 1% level. Even at the 1% level, CVEs are difficult and require visual reference charts of the type that I have published. Yet MAS claims that it is capable of performing visual estimates of "chrysotile" concentrations beyond one ten thousandth of a percent without so much as a visual

reference chart against which to compare. There is no scientific justification for this claim and certainly no methodology or validation establishing the accuracy of these visual estimates by MAS.

I describe this problem on pages 53 through 64 of **Exhibit C**.

b. Fiber Per Gram Figures Based on Inappropriate Extrapolation from Unpublished Method with No Calculated Rate of Error

Dr. Longo's unpublished "concentration" preparation technique leads to highly variable and inappropriate extrapolated quantitative results. As an example, in the February 28, 2023 Valadez Report, a sample size of 0.000017 grams was used to extrapolate to 1 gram of Baby Powder—58,824 times extrapolation. Given the 0.0003 to 0.0006% chrysotile concentration claimed, a lenient 0.5% maximum allowed error, and a sample size of 0.000017 grams, the calculated Confidence Level is less than 50%, making the False Positive error rate greater than 50%. Such an irresponsible and unheard-of False Positive error rate is totally unacceptable as part of an analytical methodology. A responsible laboratory will never adopt such a sampling scheme to make the False Positive error rate greater than 50%. And such a methodology could never pass scrutiny to become an accepted method by any standards setting organization.

I describe this problem on pages 65 through 75 of **Exhibit C**.

4. MAS's Liquid Density Sample Preparation Procedures for "Chrysotile" are Inaccurate and Unreliable

2020 - 2024 HLS Results

Date	MAS No.			Light Fraction %
2020-09-17	M71666	001	1	17.0
			2	14.6
			3	13.4
2021-05-25	M71216	001	1	24.2
			2	21.4
			3	21.3
2023-02-28	M71614	001	1	15.9
2023-10-19	M71643	001	1	19.7
2024-02-15	M71740	001	1	25.7

While I have reviewed all of the reports included in **Exhibit B**, the above table includes the weight recovery fractions reported by MAS in a handful of Johnson's Baby Powder products over a five-year span. This small group of samples is illustrative of the high degree of variation in the sample preparation procedure as well as the inability of MAS's sample preparation procedure to effectively concentrate the "chrysotile" that it claims to find in Johnson's Baby Powder.

As shown in the table above, from 2020 to 2024 over a five year span using various different sample preparation techniques as described in MAS's reports, the heavy liquid separation sample preparation procedure produced a series of extremely inconsistent light fractions ranging from 13.4% to 24.2% in talcum powder products, which further produced "chrysotile" concentrations ranging from 0.003% to 0.01%. For Baby Powder samples consisting of 99.9% talcum powder, which should be in the heavy fraction, how possible is the light fraction more than 1%? It is beyond comprehension that

those ridiculous two-digit light fraction results did not make MAS realize something was grossly wrong with each and every sample preparation procedure that it tried over the course of five years.

The extremely high degree of volatility in weight recovery is not only a result of the deficiency in MAS's sample preparation procedure but also a clear indication of the non-existence of chrysotile. There is no chrysotile to concentrate regardless of the heavy liquid density separation process used.

I describe this problem on pages 76 and 77 of **Exhibit C**.

Conclusion

For the reasons stated above, I disagree with each and every single identification of "chrysotile" in Johnson's Baby Powder made by Dr. Longo's laboratory in the reports that I have reviewed. The data presented by MAS demonstrate systematic and chronic deficiencies in almost every aspect of operation, from the equipment setup and calibration to the sampling procedure, the sample preparation processes, the execution of the analytical procedure, and reporting quantification procedure, which leads me to conclude that the laboratory is incapable of performing the most basic aspects of PLM analytical procedure let alone correctly identifying chrysotile by PLM.

The following is a summary of MAS's systematic and chronic deficiencies:

- Inability to ensure a 95% Confidence Level of quantification.
- Inability to correctly interpret dispersion staining colors.
- Inability to calibrate dispersion staining colors.
- Inability to understand the relationship between the material's refractive index and the refractive index of liquids used for measurement.
- Inability to conduct calibrated visual estimate (CVE).
- Inability to check the internal consistency of analytical data.
- Inability to correctly measure particle size under a polarized light microscope.
- Inability to correctly create scale bars.
- Inability to understand the fundamental physics principles governing the relationship between a material's refractive index and physical dimension.
- Inability to understand the fundamental geological principles governing the formation of minerals and mineral ore deposits.

I hold all of the opinions that I expressed in this report and **Exhibit C** to a reasonable degree of scientific certainty.



By: _____
Dr. Shu-Chun Su

Date: May 21, 2024

Exhibit A – Biography

National Voluntary Laboratory Accreditation Program
National Institute of Standards and Technology
Department of Commerce
USA

Dr. Shu-Chun Su

Shu-Chun Su became an NVLAP Technical Expert for the Bulk and Airborne Asbestos Programs in 1988. Since then, he has conducted close to a thousand NVLAP on-site assessments of bulk and airborne asbestos laboratories in the USA, Canada, Japan, and Korea.

Skills and Expertise

Dr. Su is an accomplished expert in general and optical mineralogy, petrography, igneous and metamorphic petrology, geochemistry, crystal chemistry, powder and single crystal X-ray crystallography, digital image analysis, and various microscopy techniques, including polarized light microscopy, scanning electron microscopy, transmission electron microscopy, infra-red micro-spectroscopy, Raman micro-spectroscopy, confocal laser scanning microscopy, etc. Dr. Su's analytical approach to derive refractive indices at various wavelengths from dispersion staining data was recognized to be "Su's Method" by Professors R. E. Stoiber and S. A. Morse at Massachusetts University, Amherst, in "Crystal Identification with the Polarizing Microscope," Springer, 358pp, 1994. By applying this method to bulk asbestos analysis, he has developed a standardized procedure for rapidly and accurately determining refractive indices of asbestos fibers using the dispersion staining technique. The procedure has been used by more than 95% of asbestos laboratories in the USA, Canada, Japan, and Korea since 1994 and was formally published in 2003.

In the area of airborne asbestos analysis, Dr. Su has developed a computer program as well as detailed d-spacing and interfacial angle tables for the six regulated asbestos minerals plus winchite, richterite, and talc to assist the indexing and interpretation of zone-axis SAED (selected area electron diffraction) patterns. It's been widely used by airborne asbestos laboratories around the world.

Education, Work History, and Relevant Work Experience

Dr. Su obtained a B.S. in Geochemistry from Peking University, China, in 1964 and worked in the Central Laboratory, Geological Survey of Gansu Province for 17 years. After earning an M.S. in Mineralogy at the Institute of Geology and Geophysics, Chinese Academy of Sciences in 1981, Dr. Su came to the U.S. to pursue graduate study in crystal chemistry, optical crystallography, and silicate mineralogy with Professors F. Donald Bloss and Paul H. Ribbe at Virginia Polytechnic Institute and State University. After completing his Ph.D. in Geology/Mineralogy in 1985, he did post-doctoral research to develop an automated refractometer and joined Hercules Incorporated in 1987. Before his retirement in 2006, he was a Senior Research Scientist and Director of the Light and Electron Microscopy Laboratory at Hercules Research Center, Wilmington, Delaware. He is a Fellow of the Mineralogical Society of America.

Rev. 2024-02-22

29 Publications Relevant To Asbestos Analysis

- 2024 Su, S.C. The Unification of Becke Line and Dispersion Staining Techniques For the Determination of Refractive Index of Non-Opaque Materials. *The Microscope*. 70:3, 99–112.
<https://doi.org/10.59082/XCLR4173>

- 2023 Su, S.C. The Calibration of Dispersion Staining Colors. *The Microscope*, 70:1, 3-21.
<https://doi.org/10.59082/HNQR9171>
- 2022 Su, S.C. The Dispersion Staining Technique and Its Application to Measuring Refractive Indices of Non-opaque Materials, with Emphasis on Asbestos Analysis, *The Microscope*, 69:2, pp 51–69;
<https://doi.org/10.59082/ZGWM6676>.
- 2022 Su, S.C. Area Percentage Charts to Aid Visual Estimation of Asbestos Concentration in Bulk Asbestos Samples. *The Microscope*, 69:4, 160-162. <https://doi.org/10.59082/RPCG4507>
- 2021 Su, S.C. Indexing and Interpretation of Zone-Axis SAED Patterns of Amphibole Asbestos Minerals in the Asbestos Analysis by Transmission Electron Microscopy. in *Asbestos and Other Elongate Mineral Particles—New and Continuing Challenges in the 21st Century*, ed. J. R. Millette and J. S. Webber (West Conshohocken, PA: ASTM International, 2021), 471–499. <https://doi.org/10.1520/STP163220200071>
- 2020 Su, S.C. A Comprehensive Suite of d-0 Look-Up Tables for Indexing Zone-Axis SAED Patterns of Amphibole Asbestos and Related Minerals. *The Microscope*, 68:3/4, 99-110, Appendix: Comprehensive Lattice Plane Spacing d and Interplanar Angle Tables of Asbestos and Talc Minerals. 888 pages
- 2014 Su, S.C. Can AHERA Bulk Asbestos Method Statistically Differentiate ACM from Non-ACM? Johnson Conference, July 21- 23, 2014. Burlington, Vermont.
- 2012 Su, S.C. Fundamental Flaws of AHERA Test Method for Determining Asbestos Concentration of Bulk Insulation Samples. Proceedings of Geological Society of America, Annual Meeting, November 4 - 7, 2012. Charlotte, North Carolina.
- 2005 Su, S.C. Analytical Sensitivity of Bulk Asbestos Analysis. Proceedings of 2005 ASTM Johnson Conference. July 18 - 22, 2005. Burlington, Vermont.
- 2005 Su, S.C. Dispersion Staining – A Versatile Complement to Becke Line Method for Refractive Index Determination. Special Supplement to *Geochimica et Cosmochimica Acta*, A727.
- 2004 Gunter, M.E., Weaver, R., Bandli, B.R., Bloss, F.D., Evans, S.H., and Su, S.C., Results from a McCrone spindle stage short course, a new version of EXCALIBR, and how to build a spindle stage. *The Microscope*, 52, 23-39.
- 2003 Su, S.C., A rapid and accurate procedure for the determination of refractive indices of asbestos minerals. *American Mineralogist*, 88, 1979-1982.
- 2001 Su, S.C., Applications of Dispersion Staining Technique in Image Analysis of Colorless Particles. Rieder, C. L., Ed., Proceedings of 59th Annual Meeting of the Microscopy Society of America, 817-818.
- 1993 Su, S.C., Determination of the refractive index of solids by dispersion staining method - An analytical approach. Rieder, C. L., Ed., Proceedings of 51st Annual Meeting of the Microscopy Society of America, 456-457.
- 1992 Su, S.C., Calibration of refractive index liquids using optical glass standards with dispersion staining technique. *The Microscope*, 40, 95-108.

- 1989 Gunter, M.E., Bloss, F.D., and Su, S.C., Computer programs for the spindle stage and double-variation method. *The Microscope*, 37, 167-171.
- 1988 Gunter, M.E., Bloss, F.D., and Su, S.C., EXCALIBR revisited. *American Mineralogist*, 73, 1481-1482.
- 1987 Peacor, D.R., Dunn, P.J., Su, S.C., and Innes, J., Ribbeite, a unit-cell twinned polymorph of alleghanyite and member of the leucophoenicite group from Kombat Mine, Namibia. *American Mineralogist*, 72, 213-216.
- 1987 Solie, D.N. and Su, S.C., An occurrence of barium-rich mica from Alaska Range. *American Mineralogist*, 72, 995-999.
- 1987 Dunn, P.J., Peacor, D.R., Ramik, R.A., Su, S.C., and Rouse, R.C., Franklinfurnaceite, a Ca-Mn-Fe³⁺-Zn layer silicate related to chlorite, from Franklin, New Jersey. *American Mineralogist*, 72, 812-815.
- 1987 Su, S.C., Bloss, F.D. and Gunter, M.E., Procedures and computer programs to refine the double variation method. *American Mineralogist*, 72, 1011-1013.
- 1987 Dunn, P.J., Peacor, D.R., Su, S.C., Wicks, F.J. and Parker, F.J., Parabrandite, the manganese analogue of talmessite, from Sterling Hill, Ogdensburg, New Jersey. *Neues Jahrbuch fur Mineralogie, Abhandlungen*, 157, 113-119.
- 1986 Su, S.C., Ribbe, P.H., and Bloss, F.D., and Warner, J.K., Optical properties of the high albite (analbite)-high sanidine solid solution series. *American Mineralogist*, 71, 1393-1398.
- 1986 Su, S.C., Ribbe, P.H., Bloss, F.D., and Goldsmith, J.R., Optical properties of single crystals in the order-disorder series low-high albite. *American Mineralogist*, 71, 1393-1398.
- 1986 Su, S.C., Ribbe, P.H., and Bloss, F.D., Alkali feldspars: Structural states determined from composition and optic axial angle 2V. *American Mineralogist*, 71, 1285-1296.
- 1986 Dunn, P.J., Peacor, D.R., Su, S.C., Nelen, J.A., and Knorrung, O. von, Johninnesite, a new sodium manganese arsenosilicate from the Kombat Mine, Namibia. *Mineralogical Magazine*, 50, 667-670.
- 1984 Su, S.C., Bloss, F.D., Extinction angles for amphiboles or pyroxenes: A cautionary note. *American Mineralogist*, 69, 399-403.
- 1984 Su, S.C., Bloss, F.D., Ribbe, P.H., and Stewart, D.B., Optic axial angle, a precise measure of Al,Si ordering in T1 tetrahedral sites of K-rich feldspars. *American Mineralogist*, 71, 1384-1392.
- 1983 Bloss, F.D., Gunter, M., Su, S.C., and Wolfe, E.H., Gladstone-Dale constant: A new approach. *Canadian Mineralogist*, 21, 93-99.

2 Book Reviews Relevant to Asbestos Analysis

- 1989 Su, S.C., *Introduction to Optical Mineralogy*, by William D. Nesse, Oxford University Press, New York, 1986, 325p. *American Mineralogist*, 74, 506.
- 1986 Su, S.C., *Optical Mineralogy*, Second Edition, by David Shelley, Elsevier Science Publishing Co., Inc., New York, 1985, 321 p. *American Mineralogist*, 71, 1060.

28 Presentations Relevant to Asbestos Analysis

- 2017 Su, S.C., Instructor, Short Course on Optical Crystallography and The Spindle Stage. University of Idaho (January 30 – February 3, Moscow, Idaho)
- 2003 Su, S.C., Instructor, Short Course on Optical Crystallography and The Spindle Stage. INTER/MICRO-03 (July 11-13, Chicago, Illinois)
- 1999 Su, S.C., Instructor, Short Course on The Spindle Stage. INTER/MICRO-99 (July 2-3, Chicago, Illinois)
- 1998 Su, S.C., Estimating the Refractive Index Difference between a Solid Particle and an Immersion Liquid. INTER/MICRO-98 (August 10-14, Chicago, Illinois)
- 1997 Su, S.C., Improve the Proficiency in Asbestos Identification by Polarized Light Microscopy. The 15th Annual Conference of the Environmental Information Association (former National Asbestos Council), March 22 - 25, Las Vegas, Nevada.
- 1996 Su, S.C., Understanding Detection Limit and Analytical Sensitivity in TEM Airborne Asbestos Analysis. NVLAP Annual Regional Meetings (East Region: October 4, Philadelphia, PA; Central Region: October 25, Minneapolis, MN; West Region: November 1, San Francisco, CA)
- 1996 Su, S.C., Back to Basics for Bulk Asbestos Analysis. NVLAP Annual Regional Meetings (East Region: October 4, Philadelphia, PA; Central Region: October 25, Minneapolis, MN; West Region: November 1, San Francisco, CA)
- 1995 Su, S.C., Improving Accuracy in Refractive Index Measurement in Bulk Asbestos Analysis. NVLAP Annual Regional Meetings (East Region: September 15, Cincinnati, OH; Central Region: October 6, Houston, TX; West Region: October 27, Los Angeles, CA).
- 1995 Su, S.C., Identifying Tremolite, Actinolite, and Anthophyllite in Bulk Asbestos Samples. NVLAP Annual Regional Meetings (East Region: September 15, Cincinnati, OH; Central Region: October 6, Houston, TX; West Region: October 27, Los Angeles, CA).
- 1995 Su, S.C., Cooke, P.M., Perkins, R.L., and Harvey, B., Analysis of Bulk Materials for Asbestos: The Problems and Solutions. Professional Development Seminars, Environmental Management '95, the 12th Annual Conference of the Environmental Information Association (former National Asbestos Council), April 22-26, Tempe, Florida.
- 1994 Su, S.C., Measuring/recording refractive indices of asbestos fibers in NVLAP accredited environmental laboratories. NVLAP Annual Regional Meetings (West Region: June 29, Seattle, WA; Central Region: July 22, Chicago, IL; East Region: August 24, Gaithersburg, MD).

- 1994 Su, S.C., Determination of refractive indices of Asbestos Minerals. INTER/MICRO-94 (July 18-21, Chicago, Illinois).
- 1993 Su, S.C., Determination of the refractive index of solids by dispersion staining method - An analytical approach. 51st Annual Meeting of the Microscopy Society of America (July 31 - August 4, Cincinnati, Ohio).
- 1990 Su, S.C., A computer program for rapidly and accurately orienting single crystals by X-ray precession method. Symposium in Honor of Professor F. Donald Bloss (July 22-25, Blacksburg, Virginia).
- 1989 Su, S.C., Application of Spindle Stage to determining the birefringence of Synthetic fibers. The 28th Annual Meeting of Eastern Analytical Symposium (September 24-29, New York City, New York).
- 1989 Instructor, Short Course on Spindle Stage and Computer Methods. August 14-18. Offered jointly by McCone Research Institute and Virginia Polytechnic Institute and State University, Blacksburg, Virginia.
- 1989 Instructor, Short Course on Immersion Methods and Crystal Optics. August 7 - 11. Offered jointly by McCrone Research Institute and Virginia Polytechnic Institute and State University, Blacksburg, Virginia.
- 1986 Instructor, Short Course on Optical Identification of Crystals and Minerals. Virginia Polytechnic Institute and State University, Blacksburg, Virginia.
- 1986 Instructor, Short Course on Spindle Stage and Computer Methods. Virginia Polytechnic Institute and State University, Blacksburg, Virginia.
- 1986 Su, S.C., Ribbe, P.H., and Bloss, F.D., Optical, X-ray and microprobe study of low plagioclase single crystals: Discriminant analysis of discontinuities. The 14th General Meeting, the International Mineralogical Association (July 13-18, Stanford, California), Abstract with Programs, p.267.
- 1986 Su, S.C., Ribbe, P.H., and Bloss, F.D., Optical properties of alkali feldspars. Invited paper for the Symposium on Optical Properties of Minerals. The 14th General Meeting, the International Mineralogical Association (July 13-18, Stanford, California), Abstract with Programs, p.240.
- 1986 Su, S.C., Ribbe, P.H. and Bloss, F.D., Alkali feldspars: structural state determined from composition and optical angle 2V. The 99th Annual Meeting of Geological Society of America, Abstracts with Programs, 18, 766.
- 1985 Instructor, Short Course on Optical Identification of Crystals and Minerals. Virginia

Polytechnic Institute and State University, Blacksburg, Virginia.

- 1985 Instructor, Short Course on Spindle Stage and Computer Methods. Virginia Polytechnic Institute and State University, Blacksburg, Virginia.
- 1985 Su, S.C., Ribbe, P.H., and Bloss, F.D., Structural states and properties of a low-high albite series of single crystal. The 98th Annual Meeting of the Geological Society of America, Abstract with Programs, 17, 729.
- 1984 Warner, J.K., Su, S.C., Ribbe, P.H., and Bloss, F.D., Optical properties of the analbite-high sanidine solid solution series. The 97th Annual Meeting of Geological Society of America, Abstract with Programs, 16, 687.
- 1983 Su, S.C., Bloss, F.D., Ribbe, P.H., and Stewart, D.B., Optical axial angle, a precise measure of Al, Si content of the T1 tetrahedral sites in K-rich alkali feldspars. The 96th Annual Meeting of Geological Society of America Abstracts with Programs, 15, 701.
- 1983 Su, S.C., Bloss, F.D., Ribbe, P.H., and Stewart, D.B., Rapid and precise optical determination of Al, Si ordering in potassic feldspars. The 3rd NATO Advanced Study Institute on Feldspars, Feldspathoids and Their Paragenesis, June 26-July 6, Rennes, France.

Exhibit B – List of MAS Reports Reviewed in Which MAS Identifies “Chrysotile” by PLM in Johnson’s Baby Powder Products

Date	MAS Project Number(s)
2/24/2020	M70484
3/6/2020	M66515 & M66516
3/18/2020	M71095
3/20/2020	M70877
4/6/2020	M71046
5/14/2020	M71095 Rev 1
9/16/2020	M71109-M71111
9/17/2020	M71166
9/23/2020	M71095 Rev 2
9/29/2020	M71166 Sup 1
12/8/2020	M71166 Sup 2
1/25/2021	M71211
2/9/2021	M71241
3/23/2021	M65329-013; M66507-001; M66508-001; M66509-001; M66513-001; M67420-001; M67420-002; M67420-004; M67420-005
4/13/2021	M71216
5/25/2021	M71228
6/4/2021	M70859
8/20/2021	M70877
3/11/2022	M71262
2/28/2023	M71614
10/19/2023	M71643
11/28/2023	M71730
2/15/2024	M71740

Exhibit C – Demonstrative Materials

**IN RE JOHNSON & JOHNSON TALCUM POWDER PRODUCTS
MARKETING, SALES PRACTICES, AND PRODUCTS LIABILITY
LITIGATION
MDL NO. 16-2738 (FLW) (LHG)
MDL Report**

Shu-Chun Su, Ph.D.

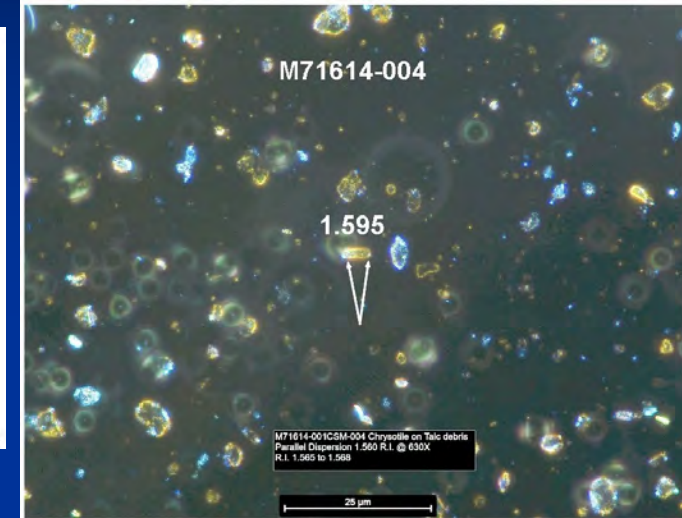
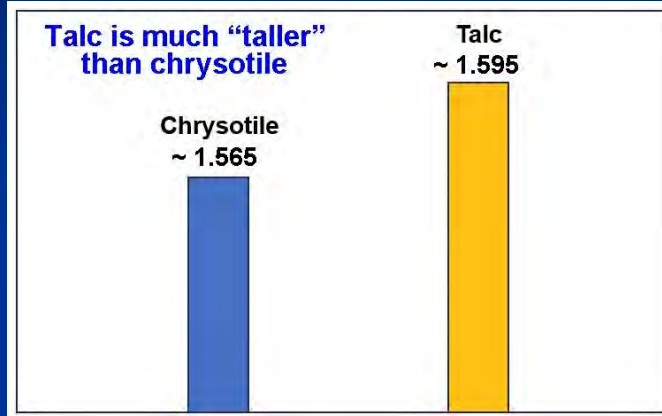
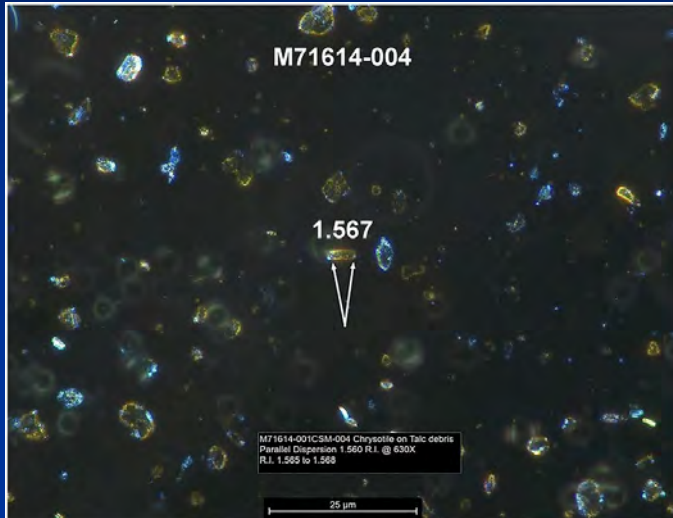
May 21, 2024

Incorrect RI Measurement Procedure: Suppressed Light Intensity

Incorrect RI Measurement Procedure

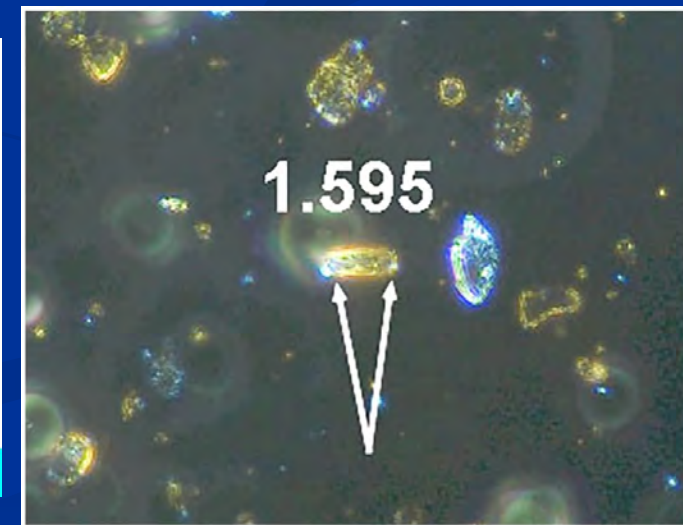
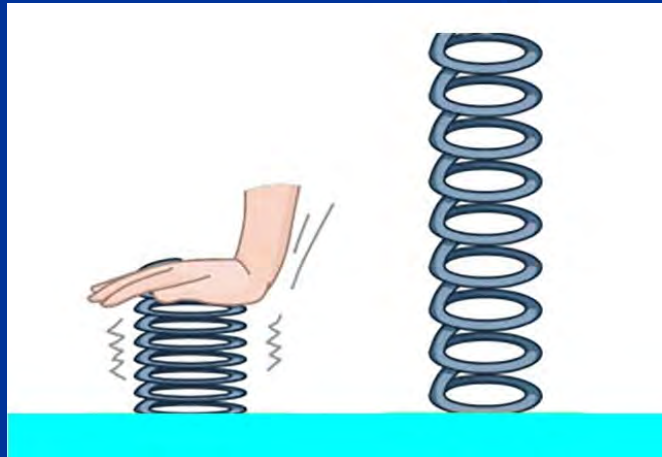
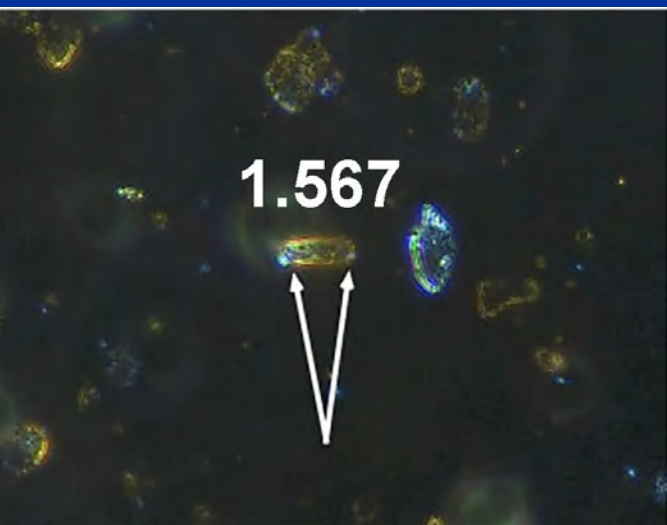
MAS Misidentified Talc as Chrysotile

2023-02-28 - Valadez Bottle Report



Suppressed

Unsuppressed



Another Example of MAS's Suppressed Illumination

Case 3:16-md-02738-MAS RLS

Document 63017-14

Filed 07/23/24

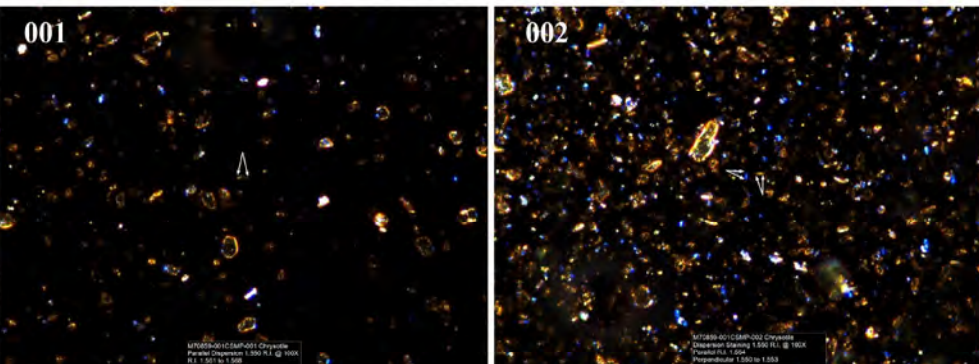
Page 25 of 50

PageID: 225096

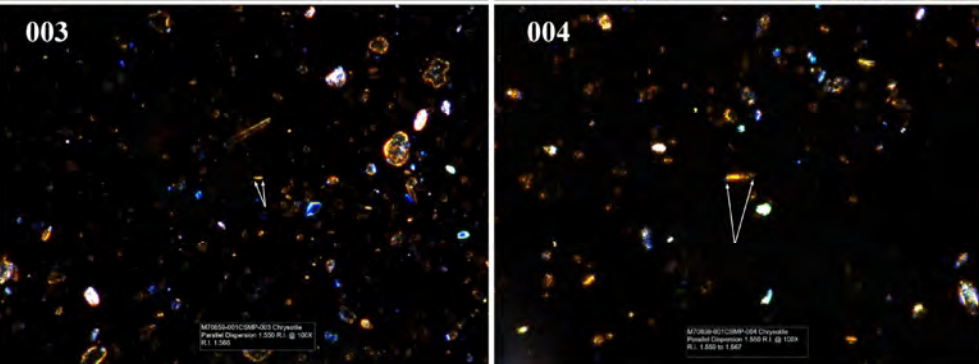
2021-06-04 M70859 JPB-UK

Original illumination was suppressed

2021-06-04 M70859-JBP-UK

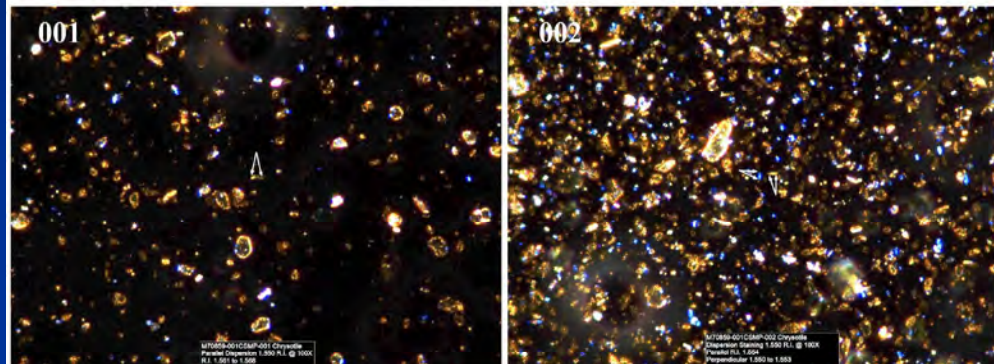


002

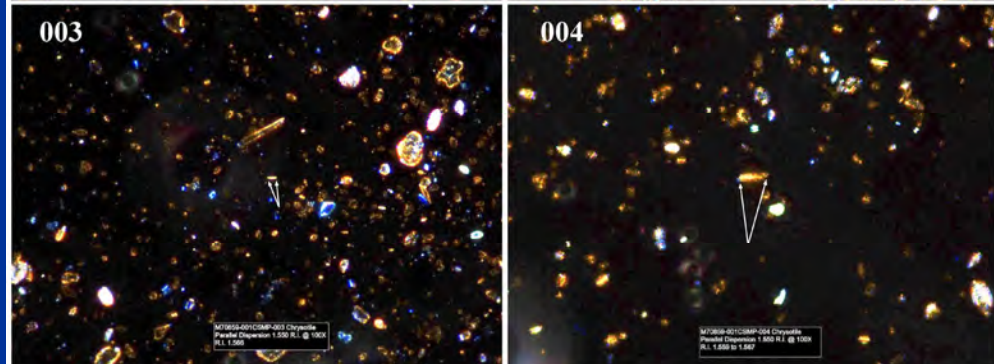


Illumination unsuppressed

2021-06-04 M70859-JBP-UK



002



Correct analysis can only be conducted when the illumination is unsuppressed.

One More Example of MAS's Suppressed Illumination

Case 3:16-md-02738-MAS-RLS

Document 33017-14

Filed 07/23/24

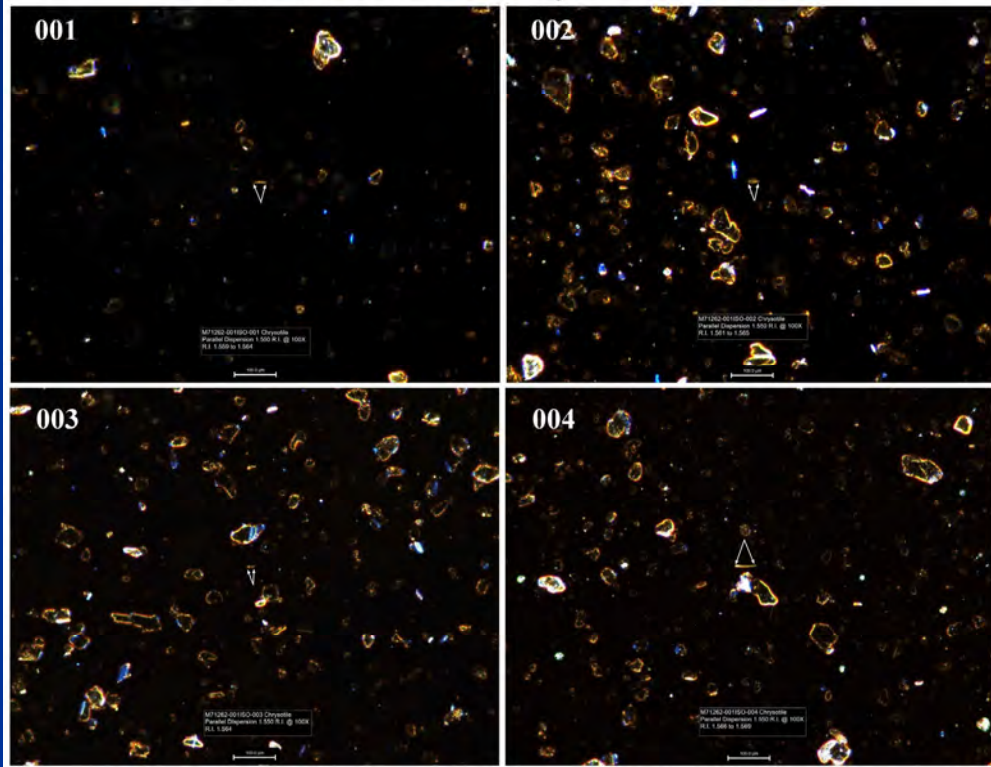
Page 26 of 50

PageID: 225097

2022-03-11 M71612 Klayman JPB & STS

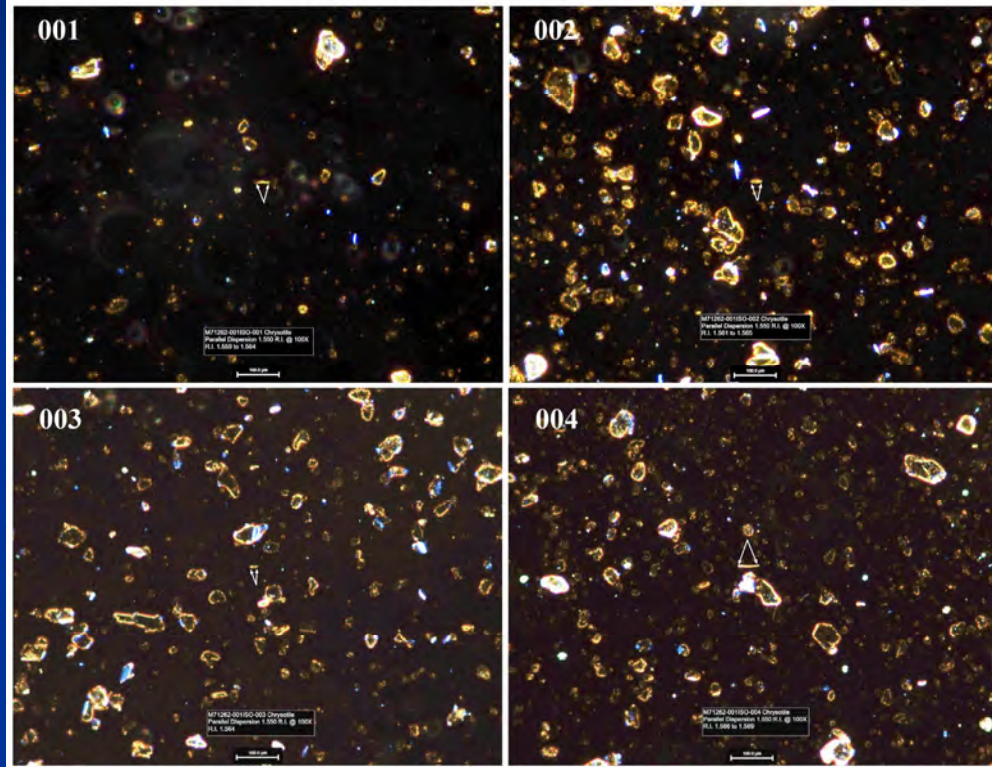
Original illumination was suppressed

2022-03-11 M71262-Klayman JPB & STS



Illumination unsuppressed

2022-03-11 M71262-Klayman JPB & STS

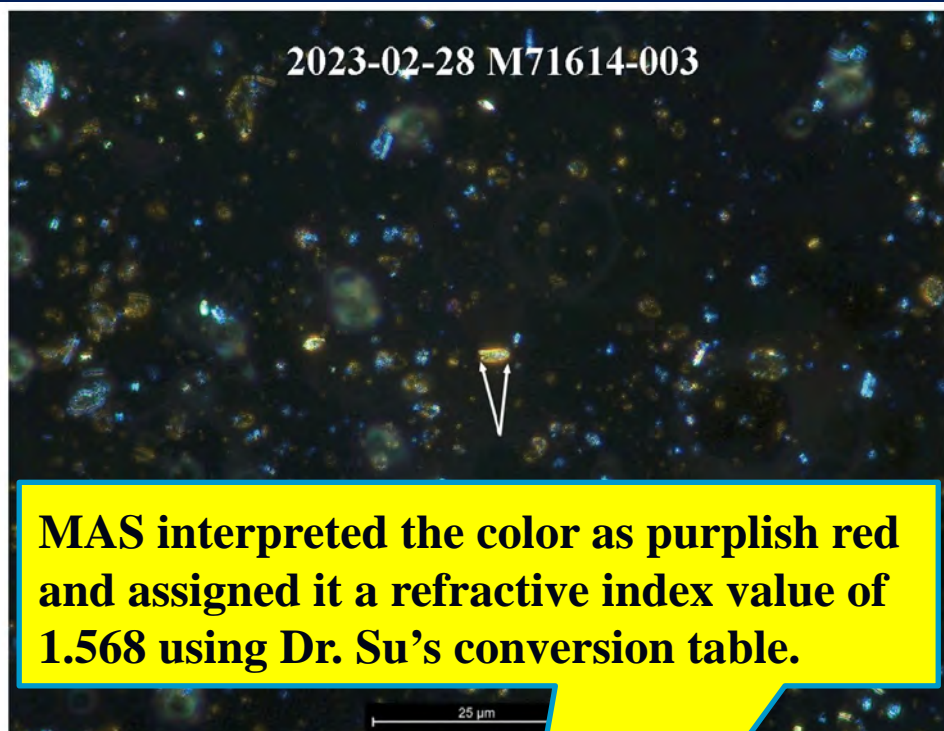
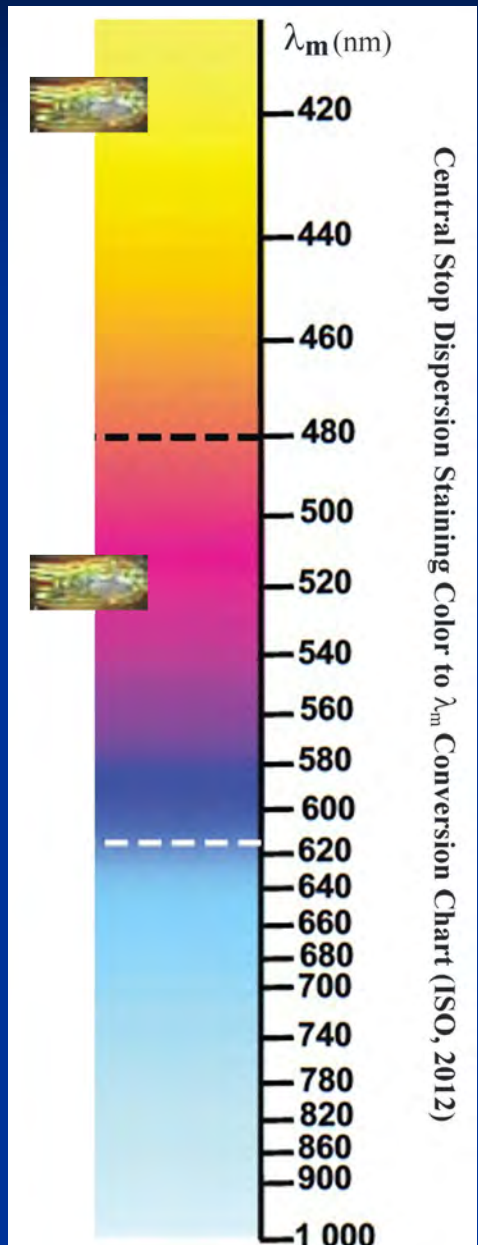


Correct analysis can only be conducted when the illumination is unsuppressed.

Incorrect RI Measurement Procedure: Inaccurate RI Values

Incorrect RI Measurement Procedure

2023-02-28 - Valadez Bottle Report



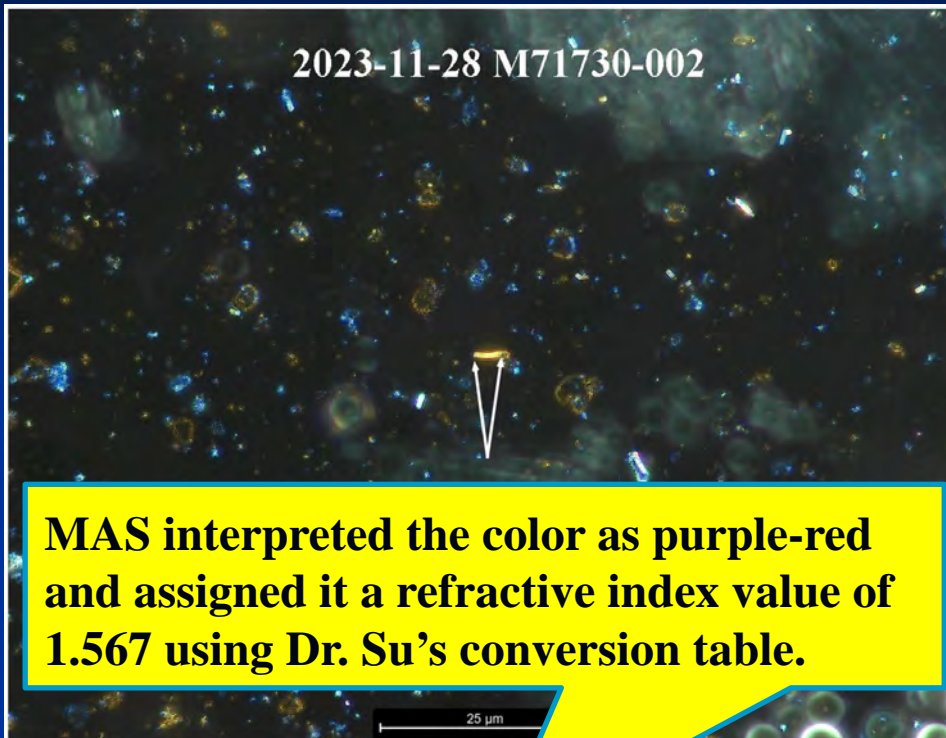
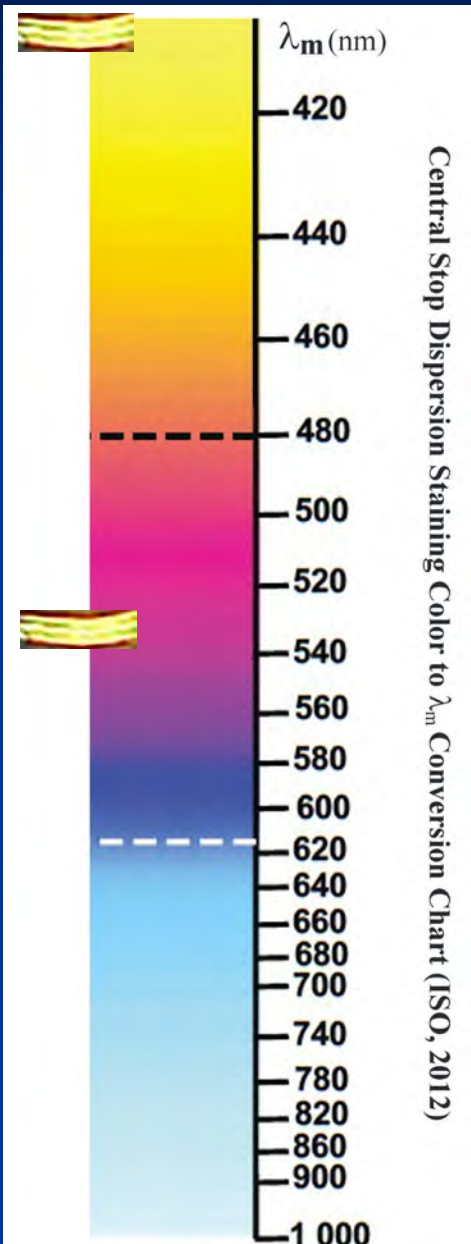
MAS interpreted the color as purplish red and assigned it a refractive index value of 1.568 using Dr. Su's conversion table.



λ_m (nm)	Matching Wavelength to RI							Cargille Liquids							Page 5 of 32								
	37°C	38°C	39°C	41°C	25°C	26°C	27°C	29°C	37°C	38°C	39°C	21°C	25°C	26°C	27°C	29°C	37°C	38°C	39°C	21°C	25°C	26°C	27°C
300	1.652	1.651	1.650	1.649	1.648	1.647	1.646	1.645	1.644	1.643	1.642	1.641	1.640	1.639	1.638	1.637	1.626	1.625	1.624	1.623	1.622	1.621	1.620
310	1.652	1.651	1.650	1.649	1.648	1.647	1.646	1.645	1.644	1.643	1.642	1.641	1.640	1.639	1.638	1.637	1.626	1.625	1.624	1.623	1.622	1.621	1.620
320	1.652	1.651	1.650	1.649	1.648	1.647	1.646	1.645	1.644	1.643	1.642	1.641	1.640	1.639	1.638	1.637	1.626	1.625	1.624	1.623	1.622	1.621	1.620
330	1.652	1.651	1.650	1.649	1.648	1.647	1.646	1.645	1.644	1.643	1.642	1.641	1.640	1.639	1.638	1.637	1.626	1.625	1.624	1.623	1.622	1.621	1.620
340	1.652	1.651	1.650	1.649	1.648	1.647	1.646	1.645	1.644	1.643	1.642	1.641	1.640	1.639	1.638	1.637	1.626	1.625	1.624	1.623	1.622	1.621	1.620
350	1.652	1.651	1.650	1.649	1.648	1.647	1.646	1.645	1.644	1.643	1.642	1.641	1.640	1.639	1.638	1.637	1.626	1.625	1.624	1.623	1.622	1.621	1.620
360	1.652	1.651	1.650	1.649	1.648	1.647	1.646	1.645	1.644	1.643	1.642	1.641	1.640	1.639	1.638	1.637	1.626	1.625	1.624	1.623	1.622	1.621	1.620
370	1.652	1.651	1.650	1.649	1.648	1.647	1.646	1.645	1.644	1.643	1.642	1.641	1.640	1.639	1.638	1.637	1.626	1.625	1.624	1.623	1.622	1.621	1.620
380	1.652	1.651	1.650	1.649	1.648	1.647	1.646	1.645	1.644	1.643	1.642	1.641	1.640	1.639	1.638	1.637	1.626	1.625	1.624	1.623	1.622	1.621	1.620
390	1.652	1.651	1.650	1.649	1.648	1.647	1.646	1.645	1.644	1.643	1.642	1.641	1.640	1.639	1.638	1.637	1.626	1.625	1.624	1.623	1.622	1.621	1.620
400	1.652	1.651	1.650	1.649	1.648	1.647	1.646	1.645	1.644	1.643	1.642	1.641	1.640	1.639	1.638	1.637	1.626	1.625	1.624	1.623	1.622	1.621	1.620
410	1.652	1.651	1.650	1.649	1.648	1.647	1.646	1.645	1.644	1.643	1.642	1.641	1.640	1.639	1.638	1.637	1.626	1.625	1.624	1.623	1.622	1.621	1.620
420	1.652	1.651	1.650	1.649	1.648	1.647	1.646	1.645	1.644	1.643	1.642	1.641	1.640	1.639	1.638	1.637	1.626	1.625	1.624	1.623	1.622	1.621	1.620
430	1.652	1.651	1.650	1.649	1.648	1.647	1.646	1.645	1.644	1.643	1.642	1.641	1.640	1.639	1.638	1.637	1.626	1.625	1.624	1.623	1.622	1.621	1.620
440	1.652	1.651	1.650	1.649	1.648	1.647	1.646	1.645	1.644	1.643	1.642	1.641	1.640	1.639	1.638	1.637	1.626	1.625	1.624	1.623	1.622	1.621	1.620
450	1.652	1.651	1.650	1.649	1.648	1.647	1.646	1.645	1.644	1.643	1.642	1.641	1.640	1.639	1.638	1.637	1.626	1.625	1.624	1.623	1.622	1.621	1.620
460	1.652	1.651	1.650	1.649	1.648	1.647	1.646	1.645	1.644	1.643	1.642	1.641	1.640	1.639	1.638	1.637	1.626	1.625	1.624	1.623	1.622	1.621	1.620
470	1.652	1.651	1.650	1.649	1.648	1.647	1.646	1.645	1.644	1.643	1.642	1.641	1.640	1.639	1.638	1.637	1.626	1.625	1.624	1.623	1.622	1.621	1.620
480	1.652	1.651	1.650	1.649	1.648	1.647	1.646	1.645	1.644	1.643	1.642	1.641	1.640	1.639	1.638	1.637	1.626	1.625	1.624	1.623	1.622	1.621	1.620
490	1.652	1.651	1.650	1.649	1.648	1.647	1.646	1.645	1.644	1.643	1.642	1.641	1.640	1.639	1.638	1.637	1.626	1.625	1.624	1.623	1.622	1.621	1.620
500	1.652	1.651	1.650	1.649	1.648	1.647	1.646	1.645	1.644	1.643	1.642	1.641	1.640	1.639	1.638	1.637	1.626	1.625	1.624	1.623	1.622	1.621	1.620
510	1.652	1.651	1.650	1.649	1.648	1.647	1.646	1.645	1.644	1.643	1.642	1.641	1.640	1.639	1.638	1.637	1.626	1.625	1.624	1.623	1.622	1.621	1.620
520	1.652	1.651	1.650	1.649	1.648	1.647	1.646	1.645	1.644	1.643	1.642	1.641	1.640	1.639	1.638	1.637	1.626	1.625	1.624	1.623	1.622	1.621	1.620
530	1.652	1.651	1.650	1.649	1.648	1.647	1.646	1.645	1.644	1.643	1.642	1.641	1.640	1.639	1.638	1.637	1.626	1.625	1.624	1.623	1.622	1.621	1.620
540	1.652	1.651	1.650	1.649	1.648	1.647	1.646	1.645	1.644	1.643	1.642	1.641	1.640	1.639	1.638	1.637	1.626	1.625	1.624	1.623	1.622	1.621	1.620
550	1.652	1.651	1.650	1.649	1.648	1.647	1.646	1.645	1.644	1.643	1.642	1.641	1.640	1.639	1.638	1.637	1.626	1.625	1.624	1.623	1.622	1.621	1.620
560	1.652	1.651	1.650	1.649	1.648	1.647	1.646	1.645	1.644	1.643	1.642	1.641	1.640	1.639	1.638	1.637	1.626	1.625	1.624	1.623	1.622	1.621	1.620
570	1.652	1.651	1.650	1.649	1.648	1.647	1.646	1.645	1.644	1.643	1.642	1.641	1.640	1.639	1.638	1.637	1.626	1.625	1.624	1.623	1.622	1.621	1.620
580	1.652	1.651	1.650	1.649	1.648	1.647	1.646	1.645	1.644	1.643	1.642	1.641	1.640	1.639	1.638	1.637	1.626	1.625	1.624	1.623	1.622	1.621	1.620
590	1.652	1.651	1.650	1.649	1.648	1.647	1.646	1.645	1.644	1.643	1.642	1.641	1.640	1.639	1.638	1.637	1.626	1.625	1.624	1.623	1.622	1.621	1.620
600	1.652	1.651	1.650	1.649	1.648	1.647	1.646	1.645	1.644	1.643	1.642	1.641	1.640	1.639	1.638	1.637	1.626	1.625	1.624	1.623	1.622	1.621	1.620
610	1.652	1.651	1.650	1.649	1.648	1.647	1.646	1.645	1.644	1.643	1.642	1.641	1.640	1.639	1.638	1.637	1.626	1.625	1.624	1.623	1.622	1.621	1.620
620	1.652	1.651	1.650	1.649	1.648	1.647	1.646	1.645	1.644	1.643	1.642	1.641	1.640	1.639	1.638	1.637	1.626	1.625	1.624	1.623	1.622	1.621	1.620
630	1.652	1.651	1.650	1.649	1.648	1.647	1.646	1.645	1.644	1.643	1.642	1.641	1.640	1.639	1.638	1.637	1.626	1.625	1.624	1.623	1.622	1.621	1.620
640	1.652	1.651	1.650	1.649	1.648	1.647	1.646	1.645	1.644	1.643	1.642	1.641	1.640	1.639	1.638	1.637	1.626	1.625	1.624	1.623	1.622	1.621	1.620
650	1.652	1.651	1.650	1.649	1.648	1.647	1.646	1.645	1.644	1.643	1.642	1.641	1.640	1.639	1.638	1.637	1.626	1.625	1.624	1.623	1.622	1.621	1.620
660	1.652	1.651	1.650	1.649	1.648	1.647	1.646	1.645	1.644	1.643	1.642	1.641	1.640	1.639	1.638	1.637	1.626	1.625	1.624	1.623	1.622	1.621	1.620
670	1.652	1.651	1.650	1.649	1.648	1.647	1.646	1.645	1.644	1.643	1.642	1.641	1.640	1.639	1.638	1.637	1.626	1.625	1.624	1.623	1.622	1.621	1.620
680	1.652	1.651	1.650	1.649	1.648	1.647	1.646	1.645	1.644	1.643	1.642	1.641	1.640	1.639	1.638	1.637	1.626	1.625	1.624	1.623	1.622	1.621	1.620
690	1.652	1.651	1.650	1.649	1.648	1.647	1.646	1.645	1.644	1.643	1.642	1.641	1.640	1.639	1.638	1.637	1.626	1.625	1.624	1.623	1.622	1.621	1.620
700	1.652	1.651	1.650	1.649	1.648	1.647	1.646</																

Incorrect RI Measurement Procedure

2023-11-28 - Henderson-Longo Sup. J&J Report



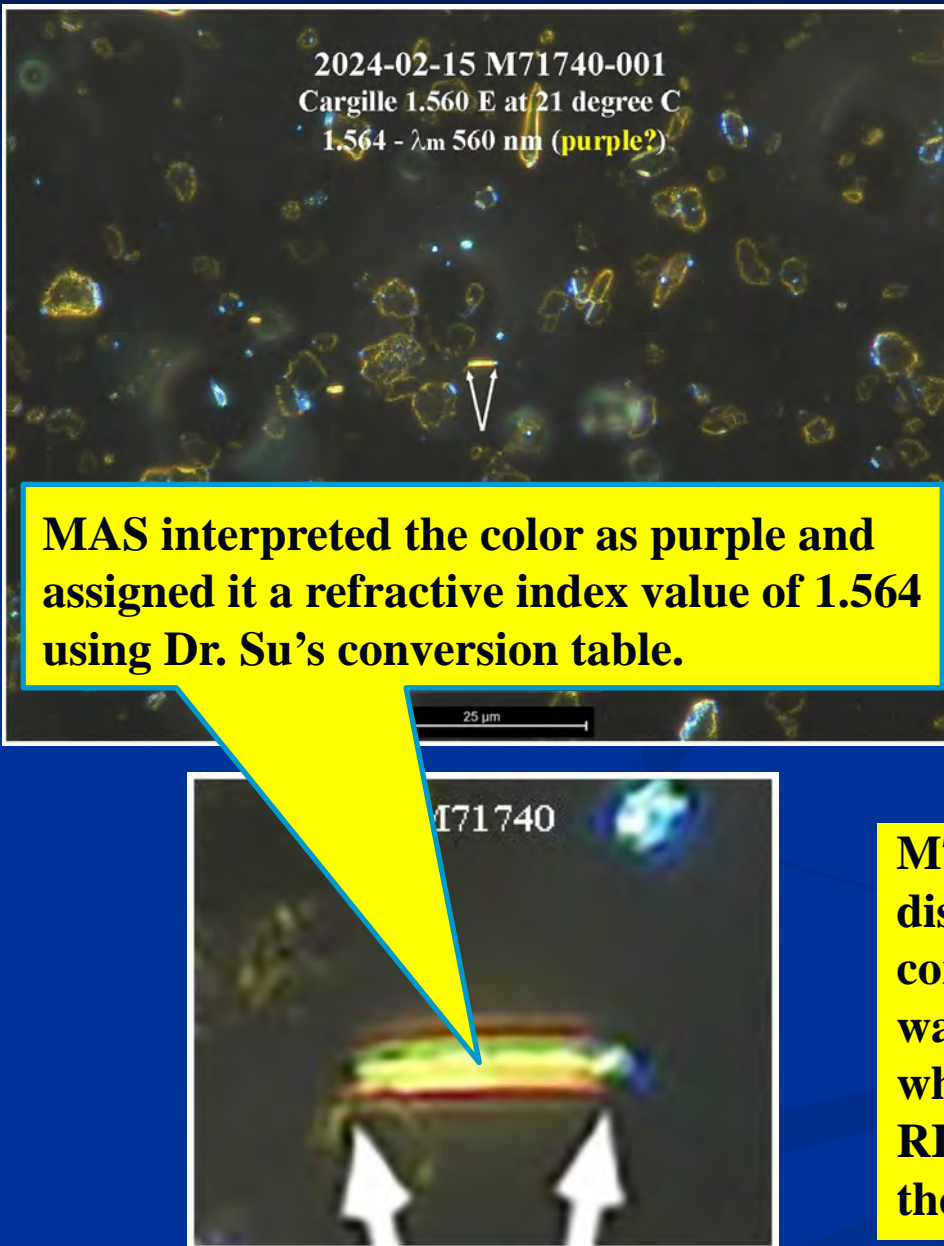
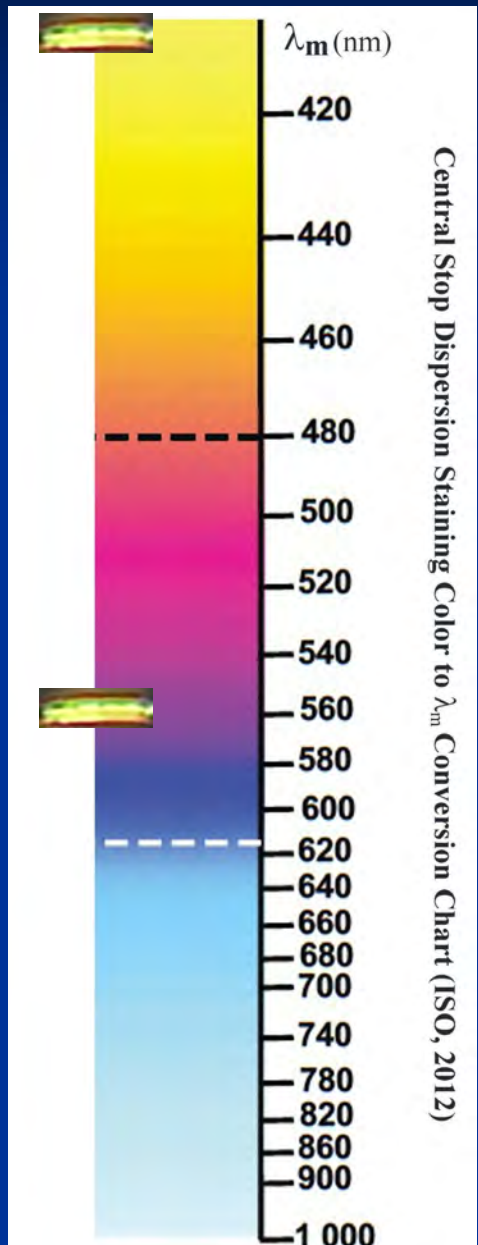
λ_m (nm)	Matching Wavelength to RI						Cargille Liquids	Page 5 of 32
	37°C	38°C	39°C	21°C	28°C	29°C		
300	1.652	1.651	1.650	1.649	1.648	1.647	1.646	1.645
310	1.652	1.651	1.650	1.649	1.648	1.647	1.646	1.645
320	1.652	1.651	1.650	1.649	1.648	1.647	1.646	1.645
330	1.652	1.651	1.650	1.649	1.648	1.647	1.646	1.645
340	1.652	1.651	1.650	1.649	1.648	1.647	1.646	1.645
350	1.652	1.651	1.650	1.649	1.648	1.647	1.646	1.645
360	1.652	1.651	1.650	1.649	1.648	1.647	1.646	1.645
370	1.652	1.651	1.650	1.649	1.648	1.647	1.646	1.645
380	1.652	1.651	1.650	1.649	1.648	1.647	1.646	1.645
390	1.652	1.651	1.650	1.649	1.648	1.647	1.646	1.645
400	1.652	1.651	1.650	1.649	1.648	1.647	1.646	1.645
410	1.652	1.651	1.650	1.649	1.648	1.647	1.646	1.645
420	1.652	1.651	1.650	1.649	1.648	1.647	1.646	1.645
430	1.652	1.651	1.650	1.649	1.648	1.647	1.646	1.645
440	1.652	1.651	1.650	1.649	1.648	1.647	1.646	1.645
450	1.652	1.651	1.650	1.649	1.648	1.647	1.646	1.645
460	1.652	1.651	1.650	1.649	1.648	1.647	1.646	1.645
470	1.652	1.651	1.650	1.649	1.648	1.647	1.646	1.645
480	1.652	1.651	1.650	1.649	1.648	1.647	1.646	1.645
490	1.652	1.651	1.650	1.649	1.648	1.647	1.646	1.645
500	1.652	1.651	1.650	1.649	1.648	1.647	1.646	1.645
510	1.652	1.651	1.650	1.649	1.648	1.647	1.646	1.645
520	1.652	1.651	1.650	1.649	1.648	1.647	1.646	1.645
530	1.652	1.651	1.650	1.649	1.648	1.647	1.646	1.645
540	1.652	1.651	1.650	1.649	1.648	1.647	1.646	1.645
550	1.652	1.651	1.650	1.649	1.648	1.647	1.646	1.645
560	1.652	1.651	1.650	1.649	1.648	1.647	1.646	1.645
570	1.652	1.651	1.650	1.649	1.648	1.647	1.646	1.645
580	1.652	1.651	1.650	1.649	1.648	1.647	1.646	1.645
590	1.652	1.651	1.650	1.649	1.648	1.647	1.646	1.645
600	1.652	1.651	1.650	1.649	1.648	1.647	1.646	1.645
610	1.652	1.651	1.650	1.649	1.648	1.647	1.646	1.645
620	1.652	1.651	1.650	1.649	1.648	1.647	1.646	1.645
630	1.652	1.651	1.650	1.649	1.648	1.647	1.646	1.645
640	1.652	1.651	1.650	1.649	1.648	1.647	1.646	1.645
650	1.652	1.651	1.650	1.649	1.648	1.647	1.646	1.645
660	1.652	1.651	1.650	1.649	1.648	1.647	1.646	1.645
670	1.652	1.651	1.650	1.649	1.648	1.647	1.646	1.645
680	1.652	1.651	1.650	1.649	1.648	1.647	1.646	1.645
690	1.652	1.651	1.650	1.649	1.648	1.647	1.646	1.645
700	1.652	1.651	1.650	1.649	1.648	1.647	1.646	1.645
710	1.652	1.651	1.650	1.649	1.648	1.647	1.646	1.645
720	1.652	1.651	1.650	1.649	1.648	1.647	1.646	1.645
730	1.652	1.651	1.650	1.649	1.648	1.647	1.646	1.645
740	1.652	1.651	1.650	1.649	1.648	1.647	1.646	1.645
750	1.652	1.651	1.650	1.649	1.648	1.647	1.646	1.645
760	1.652	1.651	1.650	1.649	1.648	1.647	1.646	1.645
770	1.652	1.651	1.650	1.649	1.648	1.647	1.646	1.645
780	1.652	1.651	1.650	1.649	1.648	1.647	1.646	1.645
790	1.652	1.651	1.650	1.649	1.648	1.647	1.646	1.645
800	1.652	1.651	1.650	1.649	1.648	1.647	1.646	1.645
810	1.652	1.651	1.650	1.649	1.648	1.647	1.646	1.645
820	1.652	1.651	1.650	1.649	1.648	1.647	1.646	1.645
830	1.652	1.651	1.650	1.649	1.648	1.647	1.646	1.645
840	1.652	1.651	1.650	1.649	1.648	1.647	1.646	1.645
850	1.652	1.651	1.650	1.649	1.648	1.647	1.646	1.645
860	1.652	1.651	1.650	1.649	1.648	1.647	1.646	1.645
870	1.652	1.651	1.650	1.649	1.648	1.647	1.646	1.645
880	1.652	1.651	1.650	1.649	1.648	1.647	1.646	1.645
890	1.652	1.651	1.650	1.649	1.648	1.647	1.646	1.645
900	1.652	1.651	1.650	1.649	1.648	1.647	1.646	1.645
910	1.652	1.651	1.650	1.649	1.648	1.647	1.646	1.645
920	1.652	1.651	1.650	1.649	1.648	1.647	1.646	1.645
930	1.652	1.651	1.650	1.649	1.648	1.647	1.646	1.645
940	1.652	1.651	1.650	1.649	1.648	1.647	1.646	1.645
950	1.652	1.651	1.650	1.649	1.648	1.647	1.646	1.645
960	1.652	1.651	1.650	1.649	1.648	1.647	1.646	1.645

Copyright: Shu-Chun Su, Ph.D. 2022

M71730-002's pale yellow dispersion staining color corresponds to a matching wavelength of **400 nm**, which is converted to an RI of 1.597, indicating it is the γ' of talc.

Incorrect RI Measurement Procedure

2024-02-15 M71740 Analysis of JBP (Rochelle Kirch) Compiled Notebook



λ_m (nm)	Matching Wavelength to RI							Cargille Liquids	Page 5 of 32
	37°C	39°C	21°C	25°C	26°C	27°C	29°C		
300	1.652	1.651	1.650	1.649	1.648	1.647	1.646	1.645	1.644
320	1.652	1.651	1.650	1.649	1.648	1.647	1.646	1.647	1.646
340	1.618	1.617	1.618	1.615	1.614	1.613	1.612	1.614	1.613
360	1.607	1.606	1.605	1.605	1.604	1.603	1.602	1.604	1.603
380	1.597	1.596	1.595	1.595	1.595	1.595	1.594	1.596	1.595
400	1.593	1.593	1.591	1.590	1.589	1.588	1.587	1.590	1.589
420	1.587	1.586	1.585	1.584	1.583	1.582	1.582	1.585	1.584
440	1.583	1.582	1.581	1.580	1.579	1.578	1.577	1.581	1.580
460	1.579	1.578	1.577	1.576	1.575	1.574	1.573	1.578	1.577
480	1.576	1.575	1.574	1.573	1.572	1.571	1.570	1.575	1.574
500	1.573	1.572	1.571	1.570	1.569	1.568	1.567	1.572	1.571
520	1.570	1.569	1.568	1.567	1.567	1.566	1.565	1.570	1.569
540	1.568	1.567	1.566	1.565	1.564	1.563	1.563	1.568	1.567
560	1.566	1.565	1.564	1.563	1.562	1.562	1.561	1.566	1.565
580	1.564	1.563	1.563	1.562	1.562	1.561	1.560	1.564	1.563
600	1.563	1.562	1.561	1.560	1.559	1.558	1.557	1.563	1.562
620	1.561	1.560	1.559	1.558	1.557	1.556	1.556	1.560	1.559
640	1.560	1.559	1.558	1.557	1.556	1.555	1.555	1.559	1.558
660	1.559	1.558	1.557	1.556	1.556	1.555	1.555	1.559	1.558
680	1.558	1.557	1.556	1.555	1.554	1.553	1.553	1.558	1.557
700	1.557	1.556	1.555	1.554	1.553	1.552	1.552	1.557	1.556
720	1.556	1.555	1.554	1.553	1.552	1.550	1.550	1.556	1.555
740	1.555	1.554	1.553	1.552	1.551	1.550	1.549	1.555	1.554
760	1.554	1.553	1.552	1.552	1.551	1.550	1.549	1.554	1.553
780	1.553	1.553	1.552	1.552	1.551	1.550	1.549	1.554	1.553
800	1.553	1.553	1.551	1.550	1.549	1.548	1.547	1.554	1.548
820	1.551	1.550	1.549	1.548	1.547	1.546	1.545	1.551	1.547
840	1.550	1.549	1.548	1.547	1.546	1.545	1.544	1.550	1.546
860	1.549	1.548	1.547	1.546	1.545	1.544	1.543	1.549	1.545
880	1.548	1.547	1.546	1.545	1.544	1.543	1.542	1.548	1.544
900	1.547	1.546	1.545	1.544	1.543	1.542	1.541	1.547	1.545
920	1.546	1.545	1.544	1.543	1.542	1.541	1.540	1.546	1.544
940	1.545	1.544	1.543	1.542	1.541	1.540	1.539	1.545	1.543
960	1.544	1.543	1.542	1.541	1.540	1.539	1.538	1.544	1.542

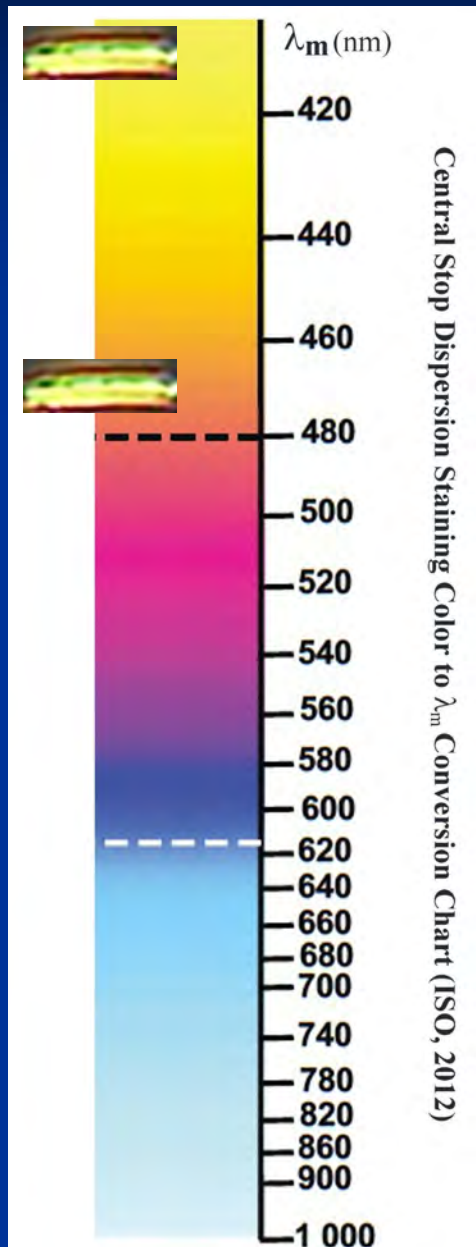
Copyright: Shu-Chun Su, Ph.D. 2022

M71740-001's pale yellow dispersion staining color corresponds to a matching wavelength of **400 nm**, which is converted to an RI of 1.597, indicating it is the γ' of talc.

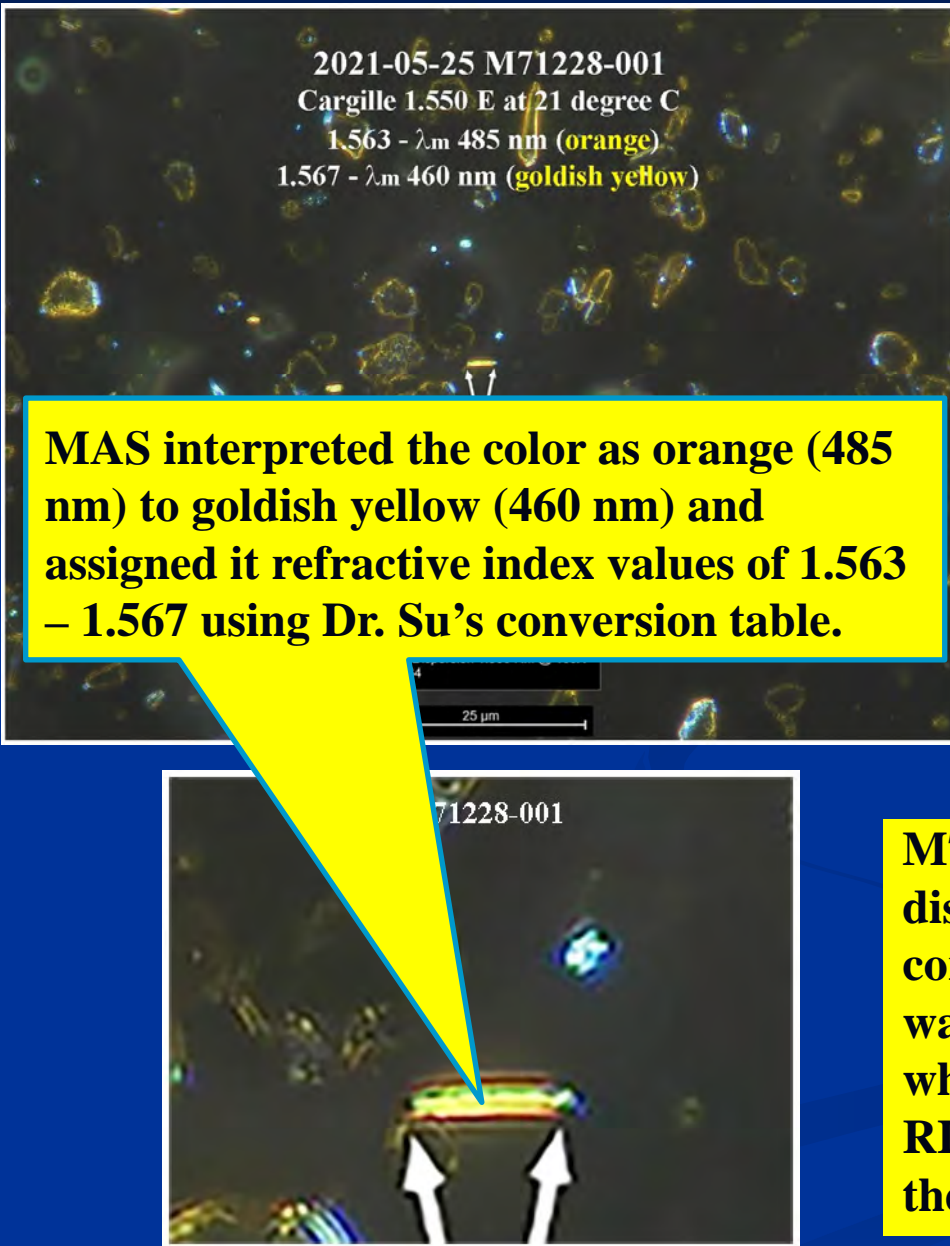
Incorrect RI Measurement Procedure: Problem Persists for Years

Incorrect RI Measurement Procedure

2021-05-25 M71228 OTShelf JBP Purchased Argentina



Central Stop Dispersion Staining Color to λ_m Conversion Chart (ISO, 2012)



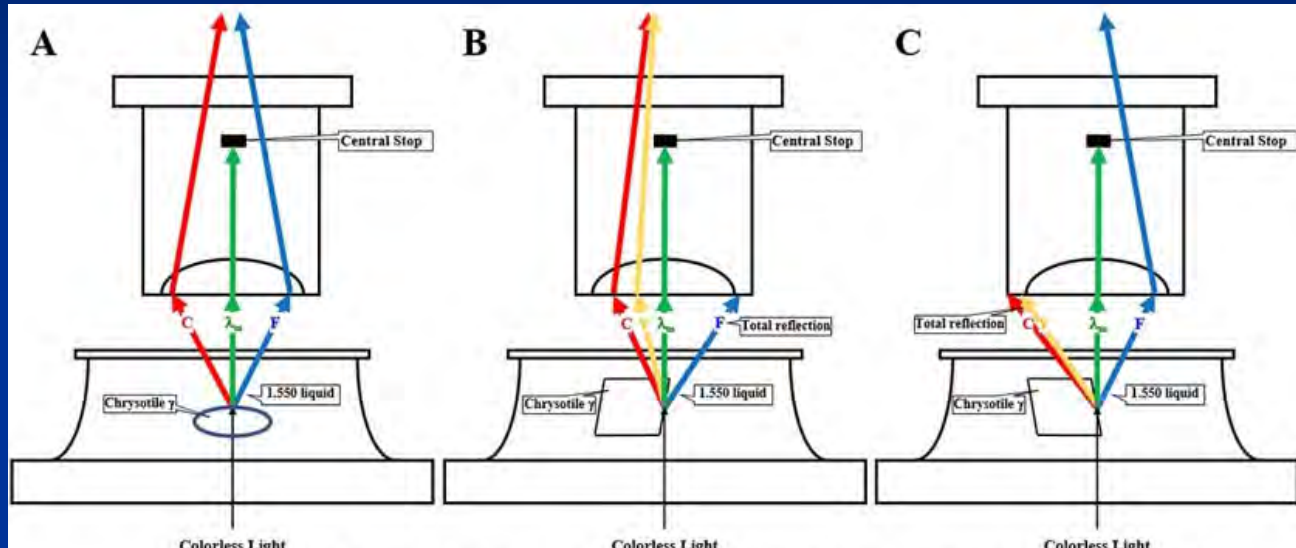
λ_m (nm)	Cargille Liquids							Chrysotile in Cargille 1.550 (E-Bulk Bottle)						
	17°C	19°C	21°C	25°C	26°C	27°C	29°C	17°C	19°C	21°C	25°C	26°C	27°C	29°C
380	1.648	1.647	1.648	1.645	1.644	1.643	1.642	1.641	1.640	1.639	1.638	1.637	1.636	1.635
390	1.637	1.636	1.635	1.634	1.633	1.632	1.631	1.632	1.631	1.630	1.629	1.628	1.627	1.626
400	1.612	1.611	1.610	1.609	1.608	1.607	1.606	1.608	1.607	1.606	1.605	1.604	1.603	1.602
410	1.592	1.591	1.590	1.589	1.588	1.587	1.586	1.593	1.592	1.591	1.590	1.589	1.588	1.587
420	1.579	1.578	1.577	1.576	1.575	1.574	1.573	1.577	1.576	1.575	1.574	1.573	1.572	1.571
430	1.574	1.573	1.572	1.571	1.570	1.569	1.568	1.573	1.572	1.571	1.570	1.569	1.568	1.567
440	1.574	1.573	1.572	1.571	1.570	1.569	1.568	1.574	1.573	1.572	1.571	1.570	1.569	1.568
450	1.570	1.569	1.568	1.567	1.566	1.565	1.564	1.570	1.569	1.568	1.567	1.566	1.565	1.564
460	1.566	1.565	1.564	1.563	1.562	1.561	1.560	1.566	1.565	1.564	1.563	1.562	1.561	1.560
470	1.561	1.560	1.559	1.558	1.557	1.556	1.555	1.560	1.559	1.558	1.557	1.556	1.555	1.554
480	1.559	1.558	1.557	1.556	1.555	1.554	1.553	1.558	1.557	1.556	1.555	1.554	1.553	1.552
490	1.557	1.556	1.555	1.554	1.553	1.552	1.551	1.556	1.555	1.554	1.553	1.552	1.551	1.550
500	1.555	1.554	1.553	1.552	1.551	1.550	1.549	1.555	1.554	1.553	1.552	1.551	1.550	1.549
510	1.553	1.552	1.551	1.550	1.549	1.548	1.547	1.553	1.552	1.551	1.550	1.549	1.548	1.547
520	1.552	1.551	1.550	1.549	1.548	1.547	1.546	1.552	1.551	1.550	1.549	1.548	1.547	1.546
530	1.551	1.550	1.549	1.548	1.547	1.546	1.545	1.551	1.550	1.549	1.548	1.547	1.546	1.545
540	1.549	1.548	1.547	1.546	1.545	1.544	1.543	1.549	1.548	1.547	1.546	1.545	1.544	1.543
550	1.548	1.547	1.546	1.545	1.544	1.543	1.542	1.548	1.547	1.546	1.545	1.544	1.543	1.542
560	1.547	1.546	1.545	1.544	1.543	1.542	1.541	1.547	1.546	1.545	1.544	1.543	1.542	1.541
570	1.546	1.545	1.544	1.543	1.542	1.541	1.540	1.546	1.545	1.544	1.543	1.542	1.541	1.540
580	1.545	1.544	1.543	1.542	1.541	1.540	1.539	1.545	1.544	1.543	1.542	1.541	1.540	1.539
590	1.544	1.543	1.542	1.541	1.540	1.539	1.538	1.544	1.543	1.542	1.541	1.540	1.539	1.538
600	1.543	1.542	1.541	1.540	1.539	1.538	1.537	1.543	1.542	1.541	1.540	1.539	1.538	1.537
610	1.542	1.541	1.540	1.539	1.538	1.537	1.536	1.542	1.541	1.540	1.539	1.538	1.537	1.536
620	1.541	1.540	1.539	1.538	1.537	1.536	1.535	1.541	1.540	1.539	1.538	1.537	1.536	1.535
630	1.540	1.539	1.538	1.537	1.536	1.535	1.534	1.540	1.539	1.538	1.537	1.536	1.535	1.534
640	1.539	1.538	1.537	1.536	1.535	1.534	1.533	1.539	1.538	1.537	1.536	1.535	1.534	1.533
650	1.538	1.537	1.536	1.535	1.534	1.533	1.532	1.538	1.537	1.536	1.535	1.534	1.533	1.532
660	1.537	1.536	1.535	1.534	1.533	1.532	1.531	1.537	1.536	1.535	1.534	1.533	1.532	1.531
670	1.536	1.535	1.534	1.533	1.532	1.531	1.530	1.536	1.535	1.534	1.533	1.532	1.531	1.530
680	1.535	1.534	1.533	1.532	1.531	1.530	1.529	1.535	1.534	1.533	1.532	1.531	1.530	1.529
690	1.534	1.533	1.532	1.531	1.530	1.529	1.528	1.534	1.533	1.532	1.531	1.530	1.529	1.528
700	1.533	1.532	1.531	1.530	1.529	1.528	1.527	1.533	1.532	1.531	1.530	1.529	1.528	1.527
710	1.532	1.531	1.530	1.529	1.528	1.527	1.526	1.532	1.531	1.530	1.529	1.528	1.527	1.526
720	1.531	1.530	1.529	1.528	1.527	1.526	1.525	1.531	1.530	1.529	1.528	1.527	1.526	1.525
730	1.530	1.529	1.528	1.527	1.526	1.525	1.524	1.530	1.529	1.528	1.527	1.526	1.525	1.524
740	1.529	1.528	1.527	1.526	1.525	1.524	1.523	1.529	1.528	1.527	1.526	1.525	1.524	1.523
750	1.528	1.527	1.526	1.525	1.524	1.523	1.522	1.528	1.527	1.526	1.525	1.524	1.523	1.522
760	1.527	1.526	1.525	1.524	1.523	1.522	1.521	1.527	1.526	1.525	1.524	1.523	1.522	1.521
770	1.526	1.525	1.524	1.523	1.522	1.521	1.520	1.526	1.525	1.524	1.523	1.522	1.521	1.520
780	1.525	1.524	1.523	1.522	1.521	1.520	1.519	1.525	1.524	1.523	1.522	1.521	1.520	1.519
790	1.524	1.523	1.522	1.521	1.520	1.519	1.518	1.524	1.523	1.522	1.521	1.520	1.519	1.518
800	1.523	1.522	1.521	1.520	1.519	1.518	1.517	1.523	1.522	1.521	1.520	1.519	1.518	1.517
810	1.522	1.521	1.520	1.519	1.518	1.517	1.516	1.522	1.521	1.520	1.519	1.518	1.517	1.516
820	1.521	1.520	1.519	1.518	1.517	1.516	1.515	1.521	1.520	1.519	1.518	1.517	1.516	1.515
830	1.520	1.519	1.518	1.517	1.516	1.515	1.514	1.520	1.519	1.518	1.517	1.516	1.515	1.514
840	1.519	1.518	1.517	1.516	1.515	1.514	1.513	1.519	1.518	1.517	1.516	1.515		

Incorrect RI Measurement Procedure

The variation of dispersion staining color is due to the total reflection



It is wrong for MAS to interpret the purple-red CSDS color at the edge as the representative color for the RI assignment because it fits the inaccurate chrysotile theory. It is a distorted CS color due to total reflection at the liquid-solid interface. The pale yellow is the right color to choose.

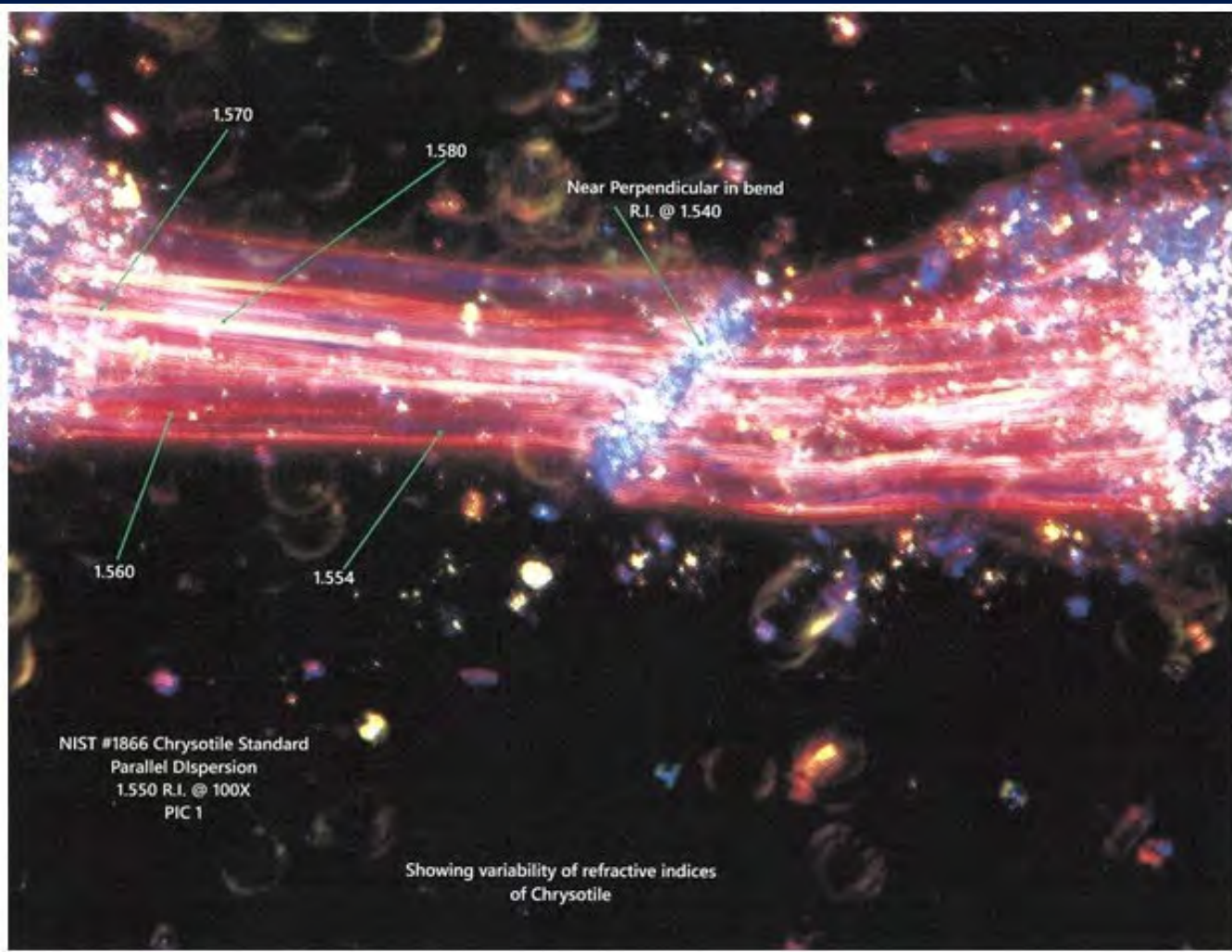


- A. Normal CSDS color. Only λ_m is blocked by the central stop. The rest of the wavelengths pass through to reach the observer's eyes.
- B. Distorted CSDS color. On top of the blocked λ_m , blue components are removed from the passing-through wavelengths due to the total reflection.
- C. Distorted CSDS color. On top of the blocked λ_m , red components are removed from the passing-through wavelengths due to the total reflection.

This image explains the physics of how total reflection occurs. By failing to consider the distortion of dispersion staining colors caused by total reflection, MAS used the wrong dispersion staining color and assigned incorrect RI values.

There is No Variability of Refractive Index within a Bundle

Case 3:16-md-02738-MAS-RLS Document 33017-14 Filed 07/23/24 Page 34 of 50
Page ID: 225105



It is wrong for MAS to interpret the variation of dispersion staining color as the variation of refractive index within the bundle.

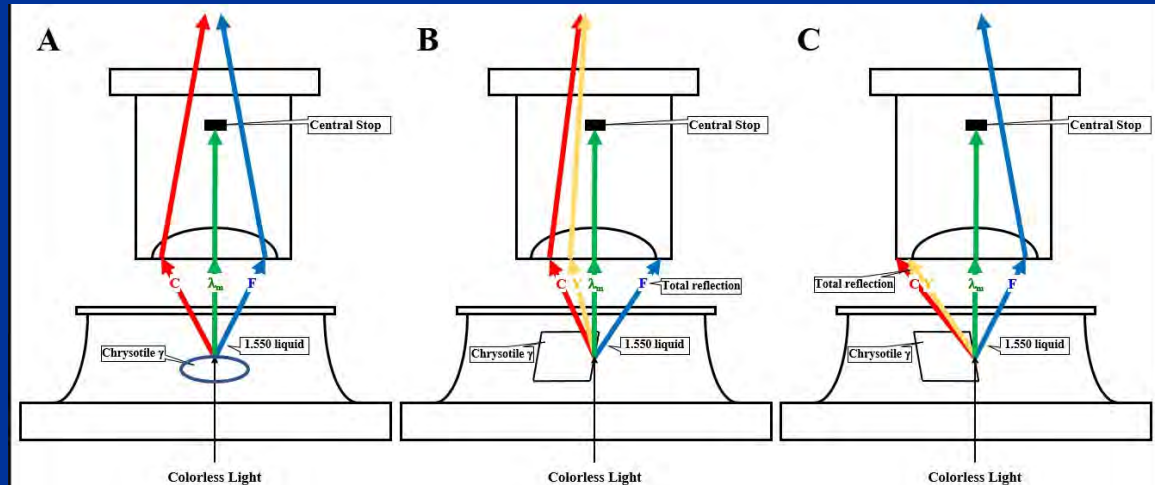
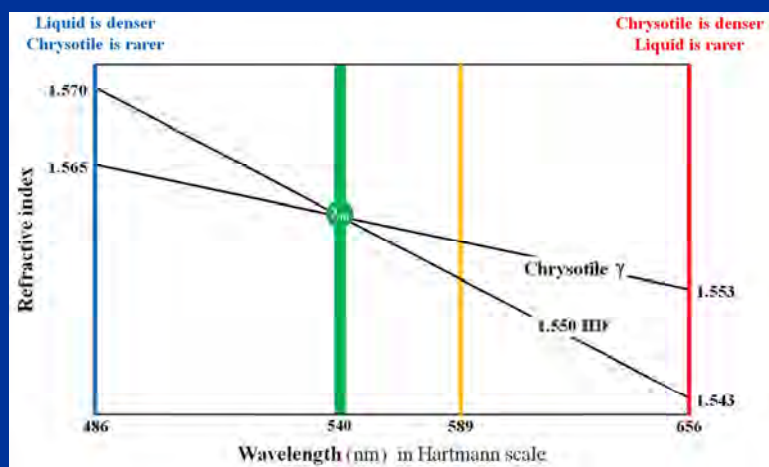
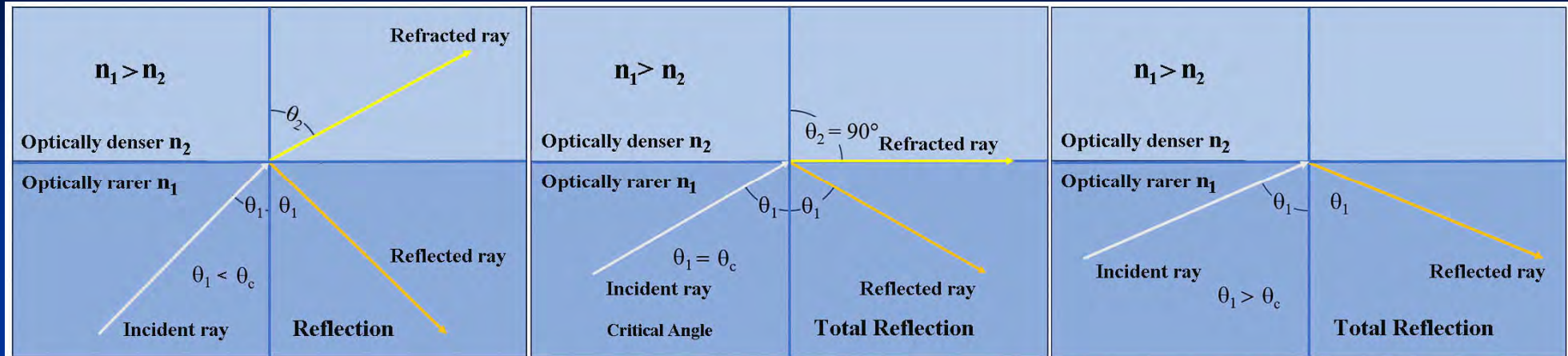
A mineral's RI is a constant governed by their chemical composition and crystal structure. MAS's theory that chrysotile's RI increases as the particle size decreases is unfounded and defies basic principles of physics. In fact, if such a theory is proved, it would shake the very foundation of physics.

The variation of dispersion staining color is caused by the total reflection occurring at the liquid-solid interface

Case 3:16-md-02738-MAS-RLS Document 33017-14 Filed 07/23/24 Page 35 of 50
 PageID: 225106

There is No Variability of Refractive Index within a Bundle

Understanding the formation of distorted dispersion staining color



λ	Color	γ	1.551 E	Critical Angle
486 nm	Blue	1.570	1.567	86.5°
656 nm	Red	1.553	1.543	83.5°

When light transmits from an optically denser (greater RI) to an optically rarer (smaller RI) medium, total internal reflection occurs at the critical angle.

The total reflection wavelengths are removed from the non-matching wavelength spectrum, resulting in the distorted dispersion staining color.

There is No Variability of Refractive Index within a Bundle

Case 3:16-md-02738-MAS-RLS Document 33017-14 Filed 07/23/24 Page 36 of 50
PageID: 225107

Table 1. Certified Values of Refractive Index for Chrysotile Asbestos in SRM 1866b

Wavelength (nm)	Lower Limit ^(a)	α		γ		
		Fitted Value	Upper Limit	Lower Limit	Fitted Value	Upper Limit
460	1.554	1.558	1.563	1.563	1.568	1.572
480	1.552	1.557	1.561	1.561	1.565	1.569
500	1.551	1.555	1.559	1.559	1.563	1.567
520	1.549	1.553	1.557	1.557	1.561	1.565
540	1.548	1.552	1.556	1.556	1.560	1.564
560	1.547	1.551	1.555	1.554	1.558	1.562
589.3	1.545	1.549	1.553	1.552	1.556	1.560
600	1.545	1.549	1.553	1.551	1.556	1.560
620	1.544	1.548	1.552	1.550	1.554	1.559
640	1.543	1.547	1.551	1.549	1.553	1.558

The certified refractive index values in the certificate issued by NIST for SRM 1866 apply to every fiber and fiber bundle in the standard reference material.

Refractive Index Does Not Change With the Particle Size

Wavelength (nm)	α			γ		
	Lower Limit ^(a)	Fitted Value	Upper Limit	Lower Limit	Fitted Value	Upper Limit
460	1.554	1.558	1.563	1.563	1.568	1.572
480	1.552	1.557	1.561	1.561	1.565	1.569
500	1.551	1.555	1.559	1.559	1.563	1.567
520	1.549	1.553	1.557	1.557	1.561	1.565
540	1.548	1.552	1.556	1.556	1.560	1.564
560	1.547	1.551	1.555	1.554	1.558	1.562
589.3	1.545	1.549	1.553	1.552	1.556	1.560
600	1.545	1.549	1.553	1.551	1.556	1.560
620	1.544	1.548	1.552	1.550	1.554	1.559
640	1.543	1.547	1.551	1.549	1.553	1.558

A mineral's RI is a constant governed by their chemical composition and crystal structure. MAS's theory that chrysotile's RI increases as the particle size decreases is unfounded and defies basic principles of physics. In fact, if such a theory is proved, it would shake the very foundation of physics.

The NIST SRM 1866 chrysotile RI values, α 1.549 and γ 1.556, were measured by John Phelps, a scientist at NIST, on a single fiber using the spindle stage technique. Dr. Longo's fibers cannot be any thinner than John Phelps's single chrysotile fiber. Dr. Longo's claim is not only unfounded but also without the support of credible measurement data.

SAMPLE 1

Sample 1 is a “pure”, short range (short fiber) chrysotile from the New Idria serpentinite body of California. The sample is white, very homogeneous, and contains very short fibers/bundles (often $< 20\mu\text{m}$) of chrysotile. The asbestosform habit of the chrysotile (and the optical properties) are best observed by viewing at high magnification (400 - 500X). The mean refractive indices are 1.560 for γ and 1.555 for α . Chrysotile comprises >95% of the sample.

Of the 257 participating laboratories, eight did not report asbestos for this sample and one reported a different asbestos type. Ten laboratories reported one or both refractive indices outside the acceptance ranges for the chrysotile. Twenty-two laboratories reported an asbestos concentration outside the acceptance range.

**The certified 1866 chrysotile RI values are α 1.549 and γ 1.556.
The certified Calidria chrysotile RI values are α 1.555 and γ 1.560.
Dr. Longo's RI values are another leap beyond the Calidria
chrysotile RI values.**

Table 5
Comparison of Chrysotile Measured Refractive Indexes Between
MAS, Dr. McCrone and Dr. Su

	Refractive Index Range Parallel	Refractive Index Range Perpendicular
MAS	ISO 1.568 to 1.561 CSM 1.568 to 1.564	ISO 1.558 to 1.550 CSM 1.556 to 1.550
Dr. McCrone	1.570 to 1.548	1.553 to 1.534
Dr. Su	1.580 to 1.540	1.579 to 1.541

MAS
misinterpreted
my table (Su,
2003)

American Mineralogist, Volume 88, pages 1979–1982, 2003

A rapid and accurate procedure for the determination of refractive indices of regulated asbestos minerals

SHU-CHUN SU*

Hercules Incorporated, Research Center, 500 Hercules Road, Wilmington, Delaware 19808, U.S.A.

ABSTRACT

By using dispersion staining methods and pre-constructed conversion tables, it is possible to quickly and accurately determine two principal refractive indices (RI) of the six regulated asbestos minerals, chrysotile, grunerite (amosite), riebeckite (crocidolite), tremolite, actinolite, and anthophyllite, in a single immersion oil mount. This procedure is especially suitable for commercial environmental laboratories specializing in the analysis of asbestos components in bulk building materials. The effectiveness of this practical procedure has been proven through rigorous testing and extensive usage over the last decade by the majority of environmental laboratories in the U.S. The principle of this procedure is also readily applicable to RI determination in other applications: mineralogy, forensics, pharmaceutical research, particle identification, etc.

MAS Misinterpreted My Table

TABLE 3. Conversion of the matching wavelength λ_0 to the corresponding RI values

Mineral	Chrysotile	Amosite	Crocidolite	Tremolite		Actinolite or Anthophyllite	
Oil $n_0^{20/20}$	1.550	1.680	1.700	1.620	1.610	1.635	1.625
Oil Series	E	B	B	E	E	E	E
RI	n_0 or n_0^2	n_0 or n_0^2					
λ_0 (nm)							
400	1.5						
420	1.5						
440	1.5						
460	1.5						
480	1.5						
500	1.5						
520	1.5						
540	1.5						
560	1.5						
580	1.5						
589	1.5						
600	1.5						
620	1.548	1.678	1.697	1.618	1.608	1.632	1.623
640	1.546	1.677	1.695	1.616	1.606	1.631	1.621
660	1.545	1.676	1.694	1.615	1.605	1.630	1.620
680	1.544	1.675	1.692	1.614	1.604	1.628	1.619
700							1.605
720							1.628
740							1.627
760							1.626
780							1.625
800							1.624
850							1.624
900							1.622
1000							1.621
Δ^L	0.0						1.618
Δ^S	0.0						0.0291
$\Delta^L - \Delta^S$	0.0						0.0127
							0.0164

Note: Temperature correction: If oil temperature is not 25°C, for every 2°C decrease/increase in temperature, add/subtract 0.001 to (from) the listed values.

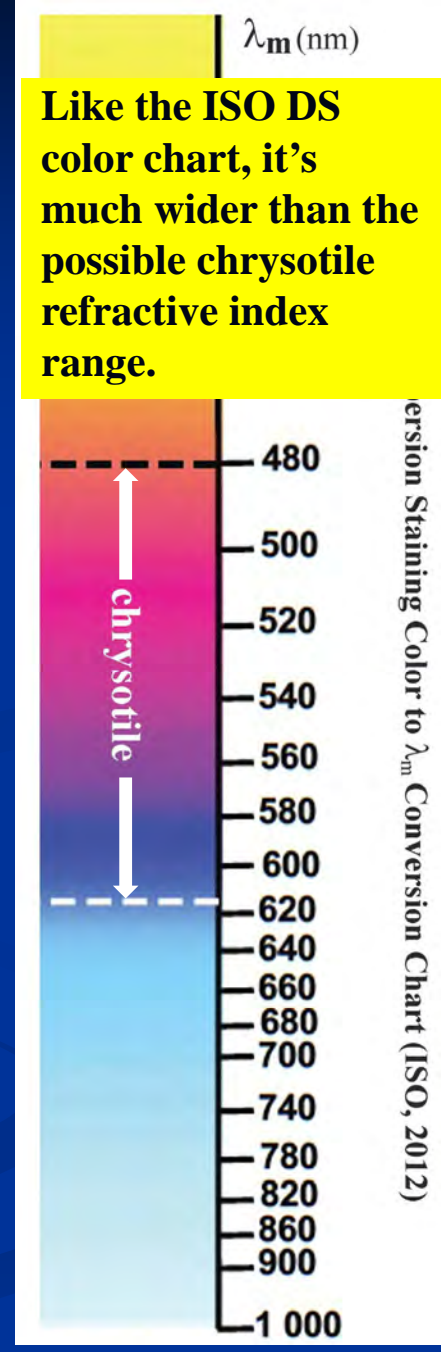
The range of each asbestos's RI values in the table must be wider than its possible minimum and maximum RI values of chrysotile or other asbestos minerals.

Table 5			
Comparison of Chrysotile Measured Refractive Indexes Between MAS, Dr. McCrone and Dr. Su			
	Refractive Index Range Parallel	Refractive Index Range Perpendicular	
MAS	ISO 1.568 to 1.561 CSM 1.568 to 1.564	ISO 1.558 to 1.550 CSM 1.556 to 1.550	
Dr. McCrone	1.570 to 1.548	1.553 to 1.534	
Dr. Su	1.580 to 1.540	1.579 to 1.541	

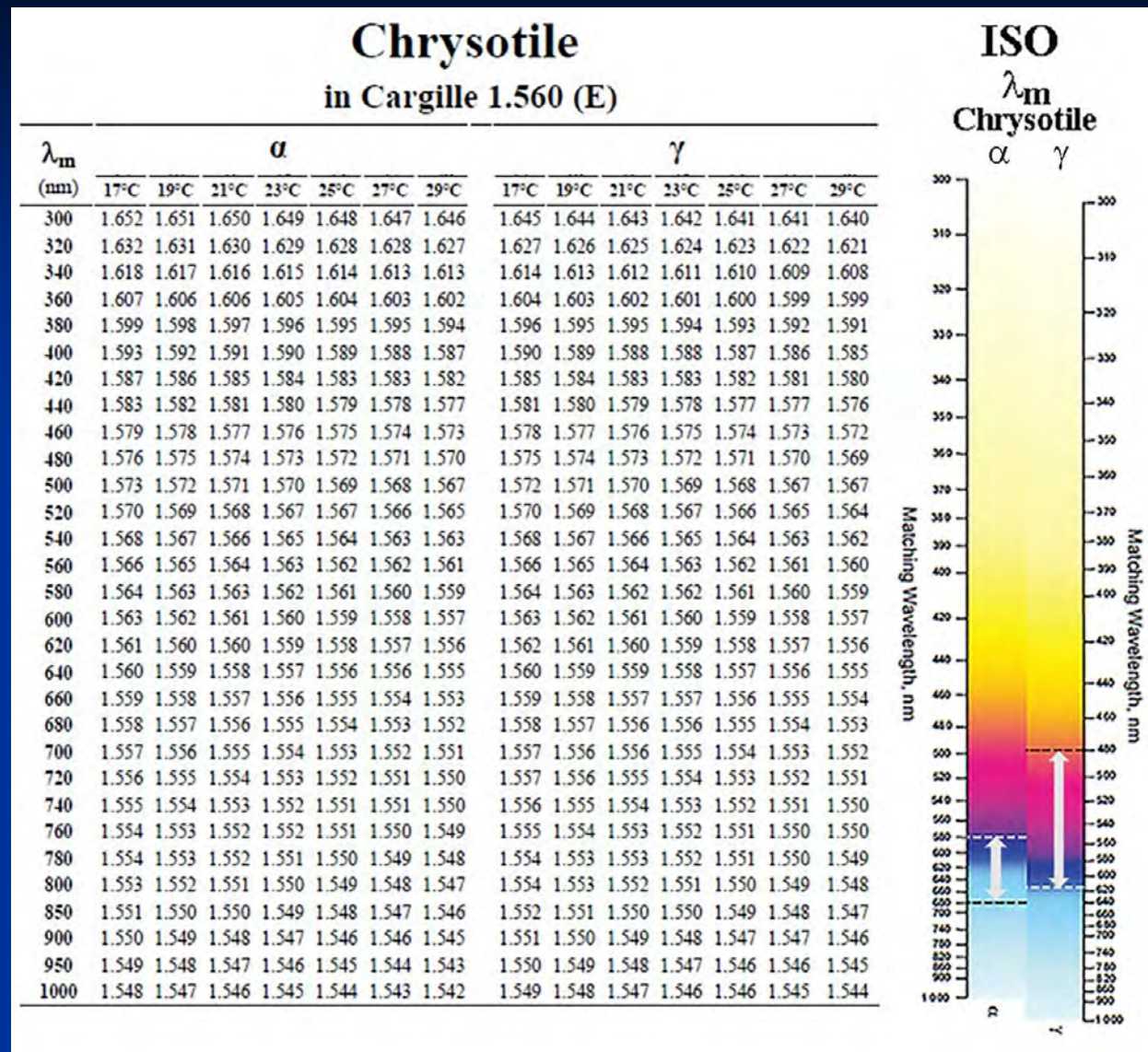
MAS misinterpreted the ranges of my table are the possible minimum and maximum values of chrysotile's refractive indices.



The kindergarten stadiometer must be taller than the possible heights of children. It doesn't mean that kindergarten students can be six feet tall.



MAS Misinterpreted My Table



Although the possible RI ranges of chrysotile α & γ are only a small section (between the dotted lines) of the CSDS color chart, the chart must cover the whole λ_m spectrum from 300 to 1000 nm. So does my conversion table. The ranges of the ISO chart and my table must be much wider than the RI range (between the dotted lines) of chrysotile. For people who understand the principle, my table is the **numerical version** of the ISO graphic chart.

Dr. Longo Misunderstood the RI Liquid's Effect on Mineral's RI

THE MICROSCOPE • Vol. 69:2 pp 51–69, 2022

The Dispersion Staining Technique and Its Application to Measuring Refractive Indices of Non-opaque Materials, with Emphasis on Asbestos Analysis

Shu-Chun Su, Ph.D.
Technical Expert, National Voluntary Laboratory Accreditation Program
National Institute of Standards and Technology⁴

3. Select a proper RI liquid to mount the sample.

Mount the suspected asbestos fibers in an appropriate RI liquid according to Table 4 DRIMMC liquid⁽¹³⁾ or 5 Cargille liquid⁽¹⁴⁾, which lists two cases: (1) for regulatory, legal, forensic, etc., which requires higher accuracy, and (2) for routine commercial analysis with less stringent accuracy requirements. For high accuracy measurement such as regulatory, legal and forensic analysis, etc., the rule of thumb is to choose RI liquids as close as possible to the RI's to be measured. For example, there are chrysotile minerals whose RI's are significantly higher than those of the standard chrysotile from the NIST SRM 1866 set. In that case, 1.555 or 1.560, instead of 1.550, RI liquids should be used to determine γ (Table 4). When efficiency is a priority and the accuracy requirement is less stringent, choose an RI liquid higher than α and lower than γ so that the two RI's can be determined in a single preparation.

In 2022, I published a paper on the application of the dispersion staining technique to asbestos analysis. I recommended the use of 1.560 RI liquid for measuring the γ of Calidria chrysotile to improve the accuracy of measurement.

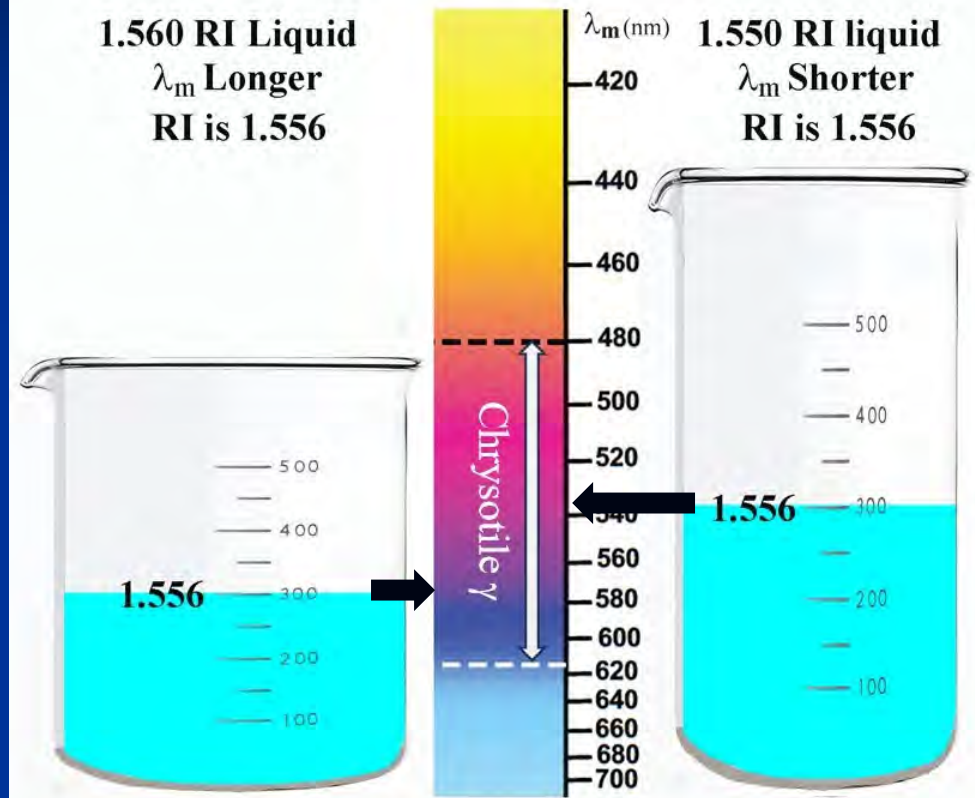
The only purpose of switching from 1.550 to 1.560 is to improve the accuracy of RI measurement because chrysotile's RI is a constant and does change with the surrounding liquid medium.

The right diagram shows two beakers, the left one is fatter, representing 1.560 liquid, and the right one is thinner, representing 1.550 liquid. The volume of water represents the γ refractive index.

When the same mineral is measured in two different RI liquids, its RI remains the same, but the matching wavelength λ_m changes accordingly: the lower liquid produces a shorter λ_m and the higher liquid produces a longer λ_m .

1.560 RI Liquid
 λ_m Longer
RI is 1.556

1.550 RI liquid
 λ_m Shorter
RI is 1.556



The right diagram shows two beakers, the left one is fatter, representing 1.560 liquid, and the right one is thinner, representing 1.550 liquid. The volume of water represents the γ refractive index. The 300 milliliters of water volume – γ value – didn't change, but the water level – λ_m – did from a shorter (upper) matching wavelength to a longer (lower) matching wavelength.

Dr. Longo Misunderstood the RI Liquid's Effect on Minerals' RI

M71614-M71643-M71740 J&J Baby Powders

Date	MAS No.			γ		α				
				Low	High	Low	High			
2023-02-28	M71614	001	1	1.564	1.564	1.561	1.561			
				2	1.565	1.565	1.561			
				3	1.568	1.568	1.557			
				4	1.565	1.568	1.560			
2023-10-19	M71643	001	1	1.566	1.566	1.561	1.561			
				2	1.566	1.569	1.557			
				3	1.561	1.561	1.552			
				4	1.568	1.568	1.559			
2024-02-15	M71740	001	1	1.564	1.564	1.560	1.560			
				2	1.564	1.564	1.560			
				3	1.565	1.565	1.562			
				4	1.563	1.563	1.561			
Average				1.565	1.565	1.559	1.560			
Grand Average				1.565		1.560				

In 2022, Dr. Longo switched to 1.560 RI liquid. Without any background in optical crystallography, Dr. Longo mistakenly thought measuring in the 1.560 liquid would increase the fiber's refractive index.

Instead of improving the accuracy of RI measurement, the 1.560 liquid produced a suite of augmented α and γ values.

The left table summarizes 12 pairs of α and γ values from M71614, M71643, and M71740.

Were those data credible (they were not), MAS single-handedly discovered a new type of chrysotile, whose refractive index is significantly higher than the Calidria chrysotile as shown in the left table.

Three Types of Chrysotile

Type	α	γ	Birefringence	RI	Source
SRM 1866	1.549	1.556	0.007	Standard	NIST
Calidria	1.555	1.560	0.005	Significantly higher than 1866	NVLAP
New?	1.560*	1.565*	0.005	Significantly higher than Calidria	MAS

* Average of 12 samples in M71614, M71643, and M71740.

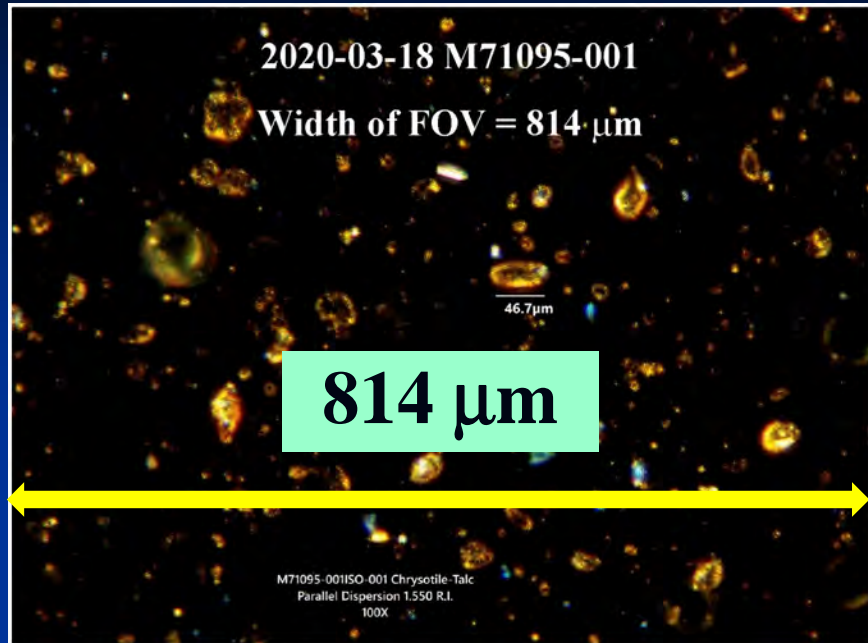
Obviously, there has never been any report of the existence of such a unique type of chrysotile with such peculiar optical properties.

Incorrect Scale Bars

Date	MAS No.	Chrysotile Length (μm)		
		Individual	Average	vs. Talc
2020-02-24 M70484	001-001	78.8	61.6	Same particle size range as talc
	001-002	33.3		
	001-003	38.5		
	001-004	71.3		
	001-005	62.2		
	001-006	57.0		
	001-007	70.4		
	001-008	49.6		
	002-001	58.5		
	002-002	78.5		
	002-003	79.3		
2020-03-18 M71095	001-001	46.7	32.2	Same particle size range as talc
	001-002	13.3		
	001-003	34.8		
	001-004	34.1		
2020-03-20 M70877	001-001	60.0	37.6	Same particle size range as talc
	001-002	25.9		
	001-003	23.0		
	001-004	41.5		
2021-05-25 M71228	001-001	105.2	55.2	Same particle size range as talc
	001-002	59.5		
	001-003	17.2		
	001-004	38.8		
2022-03-11 M71262	001-001	32.8	32.8	Same particle size range as talc
	001-002	21.6		
	001-003	26.7		
	001-004	50.0		
2023-03-28 M71614	001-001	6.0	4.9	Same particle size range as talc
	001-002	5.1		
	001-003	3.9		
	001-004	4.8		
2023-10-19 M71643	001-001	3.9	3.8	Same particle size range as talc
	001-002	6.6		
	001-003	2.2		
	001-004	2.7		
2024-02-15 M71740	001-001	3.6	8.5	Same particle size range as talc
	001-002	9.4		
	001-003	12.0		
	001-004	8.9		

Drastic variation of “chrysotile” particle size demonstrates continued inaccuracies in measuring particle sizes.

MAS's Inability to Create Scale Bars



The width of the field of view (FOV) can be calculated from the scale bar length or the width of an object.

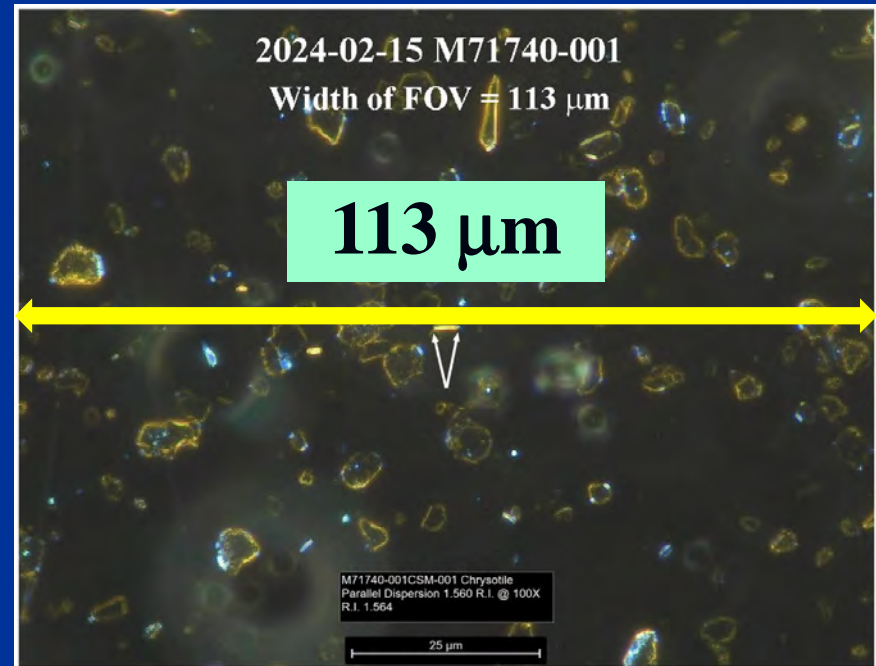
Back on 2020-03-18, the **814 μm** FOV width was wrong.

Five years later, the mistake remained uncorrected. 2024-02-15 still reported a grossly wrong FOV width of **113 μm** .

Regardless of the microscope's make, Olympus Nikon Leitz or Leica, the FOV width for a 10X objective lens is slightly over 1 mm or **1,000 μm** .

The only conclusion is that MAS is **NOT** capable of correctly performing the most fundamental operation procedure of PLM.

What is important is that talc particle sizes in these two micrographs are the same.



Incorrect Particle Size Analysis Results

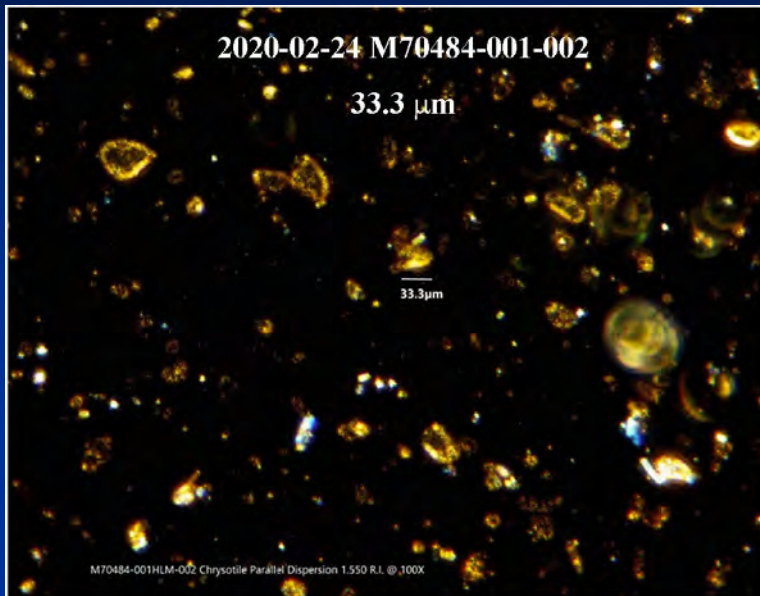
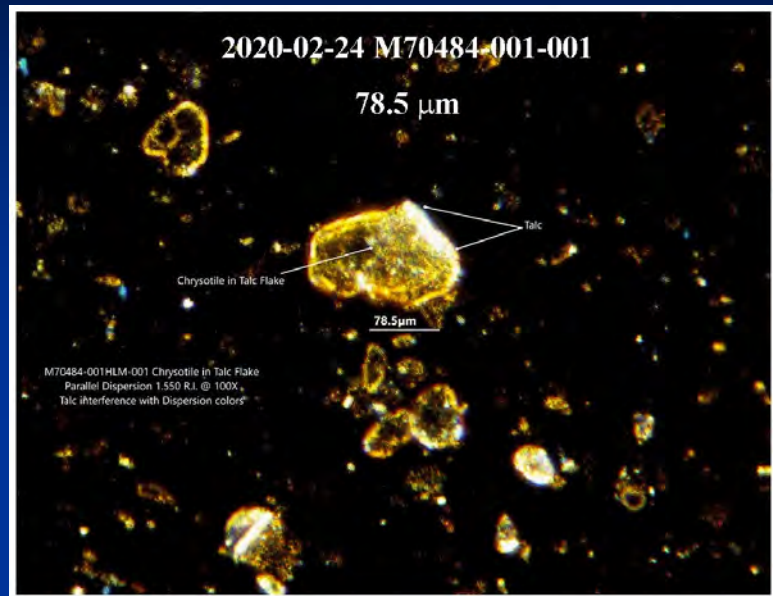
MAS's Particle Size Analysis Data

Mineral	Minimum (μm)	Average (μm)	Maximum (μm)	Reference
Talc	1.5	9.3	37.0	MAS (2017)
SG-210 Chrysotile	3.0	8.0	10.0	MAS (2023)

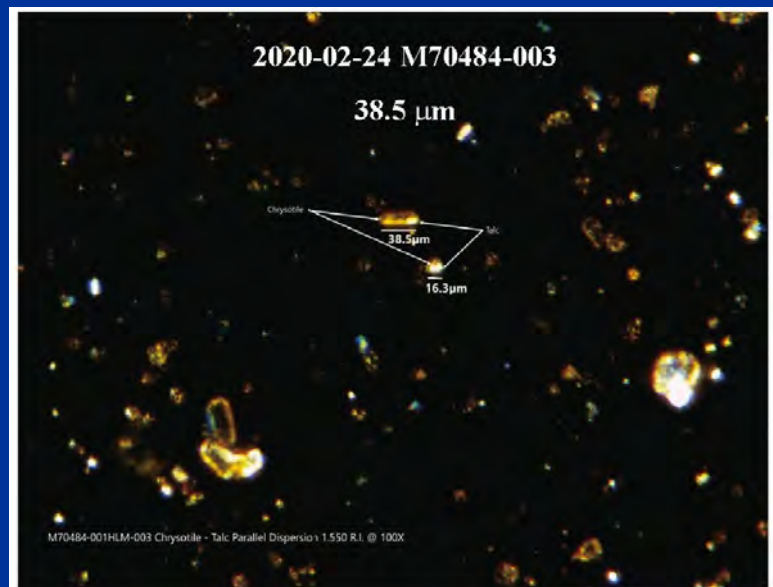
- ◆ MAS's particle size measurements in various reports do not conform to the above data.
- ◆ MAS's data do not conform to the material evidence of USP (2022) and Pier (2017)
- ◆ The maximum length of SG-210 measured by me is hundreds of micrometers, much longer than 10 micrometers by MAS.

Incorrect Particle Size Measurement Results

2020-02-24 MAS Rpt JBP-Zimmerman



All four chrysotile particles were measured and labeled by MAS.



All four chrysotile particles are similar to the particle sizes of the matrix talc particles.

Incorrect Particle Size Measurement Results

2020-02-24 MAS Rpt JBP-Zimmerman

2020-02-24 M70484-001-005

62.2 μm

62.2 μm

Transitional

M70484-001HLM-005 Chrysotile

Parallel Dispersion 1.550 R.I. @ 100X

2020-02-24 M70484-001-006

57.0 μm

57.0 μm

M70484-001HLM-006 Chrysotile
Parallel Dispersion 1.550 R.I. @ 100X

2020-02-24 M70484-001-007

70.4 μm

70.4 μm

M70484-001HLM-007 Chrysotile Parallel Dispersion 1.550 R.I. @ 100X

2020-02-24 M70484-001-008

49.6 μm

49.6 μm

M70484-001HLM-008 Chrysotile
Parallel Dispersion 1.550 R.I. @ 100X

All four chrysotile particles were measured and labeled by MAS.

All four chrysotile particles are similar to the particle sizes of the matrix talc particles.